

Distributed Fronthaul Compression and Joint Signal Recovery in Cloud-RAN

Xiongbin Rao, *Student Member, IEEE* and Vincent K. N. Lau, *Fellow, IEEE*

Abstract—The cloud radio access network (C-RAN) is a promising network architecture for future mobile communications, and one practical hurdle for its large scale implementation is the stringent requirement of high capacity and low latency fronthaul connecting the distributed remote radio heads (RRH) to the centralized baseband pools (BBUs) in the C-RAN. To improve the scalability of C-RAN networks, it is very important to take the fronthaul loading into consideration in the signal detection, and it is very desirable to reduce the fronthaul loading in C-RAN systems. In this paper, we consider uplink C-RAN systems and we propose a distributed fronthaul compression scheme at the distributed RRHs and a joint recovery algorithm at the BBUs by deploying the techniques of distributed compressive sensing (CS). Different from conventional distributed CS, the CS problem in C-RAN system needs to incorporate the underlying effect of multi-access fading for the end-to-end recovery of the transmitted signals from the users. We analyze the performance of the proposed end-to-end signal recovery algorithm and we show that the aggregate measurement matrix in C-RAN systems, which contains both the distributed fronthaul compression and multiaccess fading, can still satisfy the restricted isometry property with high probability. Based on these results, we derive tradeoff results between the uplink capacity and the fronthaul loading in C-RAN systems.

Index Terms—Cloud radio access network (C-RAN), distributed fronthaul compression, joint signal recovery, active user detection, restricted isometry property (RIP).

I. INTRODUCTION

Mobile data has been growing enormously in recent years, and to meet the increasing demand, researchers have proposed various advanced technologies to enhance the spectrum efficiency of wireless systems. In traditional cellular networks, data detection is done locally at each base station (BS), and a significant portion of the transmit power is used to overcome the path loss as well as interference from other user equipment (UEs). As a result, the cellular network is interference limited. Recently, a lot of interference mitigation techniques which exploit multi-cell cooperation (Cooperative Multi-Point (CoMP) processing) have been presented [1], [2]. However, these techniques have stringent synchronization and backhaul capacity and latency demands to exchange the channel fading states and payload among different BSs. To meet these stringent requirements, a new network architecture, namely the *cloud radio access network* (C-RAN), has been proposed [3] and it has received lots of research interest recently [4], [5]. Figure 1 illustrates a C-RAN system which consists of a number of remote radio heads (RRHs), a pool of baseband processing

units (BBUs) in the cloud as well as a high bandwidth, low latency optical transport network (fronthaul [4]) connecting the RRHs to the BBU cloud. The RRHs consist of simple low power antennas and RF components, and the baseband processing is centralized at the BBU. Such centralization offers effective CoMP interference mitigation and resource pooling gain in the cloud as well as BS virtualization [3].

Despite various attractive features of the C-RAN, one practical hurdle for its large scale implementation is the stringent requirement of high capacity and low latency fronthaul connecting the RRHs to the BBUs in the cloud. Due to the huge numbers of RRHs involved, the fronthaul is one of the most dominant cost components in C-RAN and it is very important to reduce the fronthaul loading in order to improve the scalability of C-RAN networks [5]. There are various approaches in the literature to reduce the backhaul loading in traditional cellular networks. In [6], [7], partial CoMP schemes via *sparse precoding* are proposed to reduce the backhaul consumption in cellular networks. In [8]–[11], distributed source coding strategies are used to compress the fronthaul signals in the uplink of C-RAN. By maximizing the weighted sum rate with respect to the fronthaul codebooks subject to fronthaul capacity constraint [8]–[11], the fronthaul loading in C-RAN can be effectively reduced. However, in these works [6]–[11], the uplink signal sparsity structure is ignored and the potential benefits brought by exploiting the uplink signal sparsity is not considered. In practice, the UEs' uplink packets might be sparse due to bursty transmissions of the UEs in delay-sensitive services [12] or the random access of the UEs (e.g., future machine-type communications [13] involve massive machine-type UEs with low-latency and bursty data [13]–[15]). As such, there is huge potential to exploit the uplink user sparsity to further reduce the fronthaul loading. In [16]–[18], the authors consider sparse uplink users in CDMA systems and compressive sensing (CS) recovery is deployed to improve the multi-user detection performance. However, these techniques [16]–[18] cannot be extended to the C-RAN scenarios.

In this paper, we are interested in fronthaul distributed compression using *distributed compressive sensing* and *recovery* techniques by exploiting the signal sparsity in uplink C-RAN systems. Specifically, each RRH compresses the uplink signal locally and sends it to the BBU pools in the cloud. The BBU pools then jointly recover the transmitted signals from the UEs based on the compressed uplink signals from various RRHs without knowledge of the statistics of these uplink signals. In the literature, distributed compressive sensing and recovery, in which a set of jointly sparse signals are compressively sampled

The authors are with the Department of Electronic and Computer Engineering (ECE), the Hong Kong University of Science and Technology (HKUST), Hong Kong (e-mail: {xrao, eeknlau}@ust.hk).

and then jointly recovered, have been studied in [19]. However, these existing results cannot be directly applied to the C-RAN fronthaul compression problem and there are several first order technical challenges involved.

- Distributed Fronthaul Compression and Joint Data Recovery with Multi-access Fading.** Classical distributed CS [19] concerns the joint recovery of signals that are compressed distributively at each sensor. However, these existing techniques cannot be directly applied to the C-RAN scenarios. While in C-RAN systems, the RRH locally compresses the received signals, these locally compressed signals are aggregations of the multi-user signals transmitted by different UEs over *multi-access fading*, as illustrated in Figure 2. The target of the joint recovery in the C-RAN scenarios are the *transmitted signals* from the UEs rather than the locally received signals in the RRH (as in conventional distributed CS [19]), as illustrated in Figure 2. As a result, a new distributed CS problem formulation and recovery that incorporate the effects of multi-access fading in C-RAN, is needed.
- Robust CS Recovery Conditions with Multi-access Fading.** In the literature, the restricted isometry property (RIP) [20] is commonly adopted to provide a sufficient condition for robust CS recovery [21], and it is highly non-trivial to establish a sufficient condition for the RIP of the associated measurement matrix. Note that the RIP characterizations are known for sub-sampled Fourier transformation matrices and random matrices with i.i.d. sub-Gaussian entries [21]. However, due to the complicated multi-access fading channels between the UE and the RRHs in C-RAN systems, the associated *aggregate* CS measurement matrix does not belong to any of the known measurement matrix structures, and hence, conventional results about the RIP condition cannot be applied and a new characterization of the sufficient conditions for robust CS recovery (embracing multi-access fading) will be needed for C-RAN.
- Tradeoff Analysis between C-RAN Performance and the Fronthaul Loading.** Besides applying CS in the signal recovery to achieve fronthaul compression, it is also very important to quantify the closed-form tradeoff between the capacity of the C-RAN and the fronthaul loading at each RRH. This tradeoff result will be important to reveal design insights and guidelines on the dimensioning of the fronthaul (e.g., how large a fronthaul is needed to achieve a certain capacity target in the C-RAN). However, the closed form performance analysis will be very challenging.

In this paper, we shall address the above challenges. We first introduce the uplink C-RAN model and propose a distributed fronthaul compression scheme at the RRHs of the C-RAN. We propose a joint signal recovery scheme at the BBU pools, which exploits the underlying signal sparsity of the UEs and the multi-access fading effects between the UEs and the RRHs. Based on that, we analyze the associated CS measurement matrix and show that the RIP condition [20] can be satisfied with

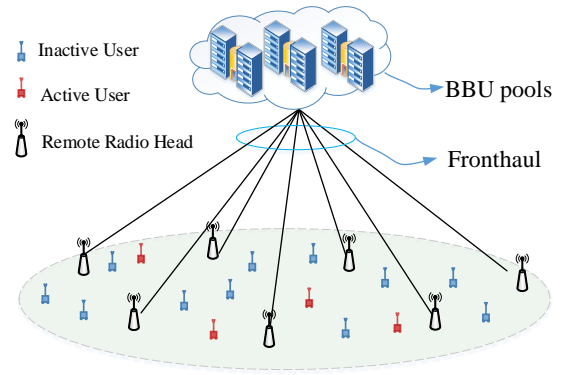


Figure 1. Illustration of a C-RAN system. The active user and inactive user, refer to the UEs that are transmitting signal and keeping silent, respectively, in the considered time slot.

high probability under some mild conditions. Furthermore, we characterize the achievable uplink capacity in terms of the compression rate on the fronthaul. From the results, we draw simple conclusions on the tradeoff relationship between the uplink C-RAN performance and the fronthaul loading in the C-RAN. Finally, we verify the effectiveness of the proposed distributive fronthaul compression scheme via simulations.

Notations: Uppercase and lowercase boldface letters denote matrices and vectors respectively. The operators $(\cdot)^T$, $(\cdot)^*$, $(\cdot)^H$, $(\cdot)^\dagger$, $\#\|\cdot\|$, $\text{tr}(\cdot)$, $O(\cdot)$ and $\text{Pr}(\cdot)$ are the transpose, conjugate, conjugate transpose, Moore-Penrose pseudoinverse, cardinality, trace, big-O notation, and probability operator respectively; $\mathbf{A}(q, p)$ and $\mathbf{a}(l)$ denote the (q, p) -th entry of \mathbf{A} and the l -th entry of \mathbf{a} respectively; \mathbf{A}_Ω and \mathbf{a}_Ω denote the sub-matrices formed by collecting the columns of \mathbf{A} and sub-vector formed by collecting the entries of \mathbf{a} , respectively, whose indexes are in set Ω ; $\|\mathbf{a}\|_q$ is the l_q -norm of the vector \mathbf{a} and is defined as $\|\mathbf{a}\|_q = \sqrt[q]{\sum_i |\mathbf{a}(i)|^q}$; and $\|\mathbf{A}\|_F$, $\|\mathbf{A}\|$ and $\|\mathbf{a}\|$ denote the Frobenius norm, spectrum norm of \mathbf{A} and Euclidean norm of vector \mathbf{a} respectively.

II. SYSTEM MODEL

A. C-RAN Topology

Consider an *uplink* C-RAN system with M distributed single-antenna RRHs where the RRHs are connected to the BBU pools via the fronthaul, as illustrated in Figure 1. There are a total of KN_c single-antenna UEs being served on N_c subcarriers and each subcarrier is allocated to K UEs. Denote the k -th UE on the c -th subcarrier as the (c, k) -th UE, and the whole set of UEs as $\mathcal{U} = \{(c, k) : c \in \{1, 2, \dots, N_c\}, k \in \{1, 2, \dots, K\}\}$. Denote $H_{ik}^{[c]} \in \mathbb{C}$ as the channel¹ from the (c, k) -th UE to the i -th RRH. The received symbol at the i -th RRH on the c -th subcarrier $y_i^{[c]}$ can be expressed as

$$y_i^{[c]} = \sum_{k=1}^K H_{ik}^{[c]} x_k^{[c]} + n_i^{[c]}, \quad i \in \{1, \dots, M\}, c \in \{1, 2, \dots, N_c\}, \quad (1)$$

where $x_k^{[c]}$ is the transmitted signal by the (c, k) -th user and $n_i^{[c]}$ is the standard complex Gaussian noise at the i -th RRH on the c -th subcarrier.

¹In $H_{ik}^{[c]}$, $i \in \{1, \dots, M\}$, $c \in \{1, \dots, N_c\}$ and $(c, k) \in \mathcal{U}$ denote the RRH index, subcarrier index, and the UE index respectively. Note that we shall frequently use this notation rule in the entire paper.

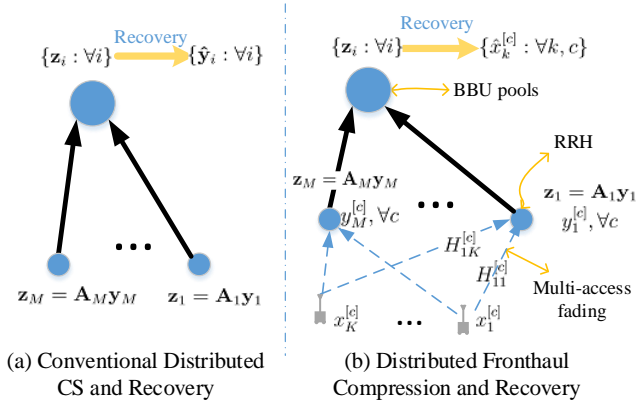


Figure 2. Illustration of conventional distributed CS and recovery [19], [22] *versus* the distributed fronthaul compression and signal recovery of C-RAN systems. Conventional distributed CS aims to recover the vectors $\{y_i\}$ that are compressively and distributively sampled. On the other hand, in C-RAN systems, the BBU pools aim to jointly recover the *transmitted signal* $\{x_k^{[c]} : \forall k, c\}$ from the UEs based on the distributively compressed data $z_i = A_i y_i, \forall i$ on the fronthaul.

Concatenate the received symbols $\{y_i^{[c]} : \forall c\}$ and the noise terms $\{n_i^{[c]} : \forall c\}$ at the i -th RRH as $\mathbf{y}_i = [y_i^{[1]} \dots y_i^{[N_c]}]^T \in \mathbb{C}^{N_c \times 1}$ and $\mathbf{n}_i = [n_i^{[1]} \dots n_i^{[N_c]}]^T \in \mathbb{C}^{N_c \times 1}$ respectively, and the transmitted symbols $\{x_k^{[c]} : \forall (c, k) \in \mathcal{U}\}$ from all the UEs as

$$\mathbf{x} = [x_1^{[1]} \dots x_K^{[1]}, \dots, x_1^{[N_c]} \dots x_K^{[N_c]}]^T \in \mathbb{C}^{KN_c \times 1}. \quad (2)$$

The signal model (1) can be re-written as

$$\mathbf{y}_i = \mathbf{H}_i \mathbf{x} + \mathbf{n}_i, \quad i \in \{1, 2, \dots, M\}, \quad (3)$$

where \mathbf{H}_i is the aggregate channel matrix from the set of UEs \mathcal{U} to the i -th RRH on N_c subcarriers and is given by

$$\mathbf{H}_i = \begin{bmatrix} H_{i1}^{[1]} & \dots & H_{iK}^{[1]} & \mathbf{0} & \dots & \mathbf{0} \\ \mathbf{0} & \dots & \mathbf{0} & \ddots & \dots & \mathbf{0} \\ \mathbf{0} & \dots & \mathbf{0} & H_{i1}^{[N_c]} & \dots & H_{iK}^{[N_c]} \end{bmatrix} \in \mathbb{C}^{N_c \times KN_c}. \quad (4)$$

We first have the following assumption on the channel model, which includes both the small scale fading and the large scale path gain process.

Assumption 1 (Channel Model): The channel $H_{ik}^{[c]}$ is given by $H_{ik}^{[c]} = g_{ik}^{[c]} h_{ik}^{[c]}$, where $g_{ik}^{[c]} \in \mathbb{R}^+$ and $h_{ik}^{[c]} \in \mathbb{C}$ denote the large scale fading and small scale fading parameters, respectively, from the (c, k) -th user to the i -th RRH.

- **Small Scale Fading:** The small fading parameters $\{h_{ik}^{[c]} : \forall i, k, c\}$ are i.i.d. standard complex Gaussian variables with zero mean and unit variance and are independent of $\{g_{ik}^{[c]} : \forall i, k, c\}$.
- **Large Scale Fading:** Let $\mathbf{g}_k^{[c]} = [\dots g_{ik}^{[c]} \dots]_{i \in \{1, \dots, M\}}$ be the large scale fading parameters from the (c, k) -th user to the set of RRHs $\{1, \dots, M\}$ and $\mathbf{g}_k^{[c]}$ is supposed to be normalized so that $\|\mathbf{g}_k^{[c]}\|_F^2 = M$. Then, $\mathbf{g}_k^{[c]}$ and $\mathbf{g}_{k'}^{[c]}$ are independent $\forall (c, k) \neq (c', k')$. Furthermore, $g_{ik}^{[c]} \in [0, \bar{g}]$ is randomly

distributed with unit second order moment, i.e., $\mathbb{E}(|g_{ik}^{[c]}|^2) = 1, \forall c, k$. ■

Note that the effect of normalization of $\mathbf{g}_k^{[c]}$ is incorporated in the different transmit SNR P_i for the active UEs as in (5). On the other hand, after the normalization, i.e., $\sum_{i=1}^M (g_{ik}^{[c]})^2 = M$, we still have the freedom to assume that the random large scale fading parameters satisfy $\mathbb{E}(|g_{1k}^{[c]}|^2) = \mathbb{E}(|g_{2k}^{[c]}|^2) = \dots = \mathbb{E}(|g_{Mk}^{[c]}|^2) = 1$ from the *uniform* geometric distributions of the users and deployments of the RRHs. The BBU is assumed to have perfect knowledge of the channel state information $\{H_{ik}^{[c]} : \forall i, k, c\}$ and this can be achieved using uplink reference signals² from the UEs [23].

From (3), the transmitted symbol vector \mathbf{x} from all the UEs has a full dimension of KN_c . However, in practice, the wireless systems might not be fully loaded and \mathbf{x} might be sparse (e.g., due to the random access mode or the massive bursty traffic of the UEs [12], [13], [24]). We illustrate two example scenarios in which the uplink UEs signals are sparse below. Some other application scenarios that involve sparse user signals can also be found in [25].

- **Sparse Uplink Signals with Machine Type UEs** [13]–[15]: Suppose the set of KN_c machine-type UEs (MTC) [13] access the network independently using random access channel (RACH) [15] and the accessing probability of each MTC user is p ($p \ll 1$ for stability [13]). Then the average number of active UEs on the uplink per time slot is $pKN_c \ll KN_c$, and hence the uplink signals tend to be sparse.
- **Sparse Uplink Signals with Bursty Applications** [12], [24]: Suppose the set of KN_c UEs is running delay-sensitive applications [12], [24] and the inter-arrival time between two data packets from each user follows from an exponential distribution with mean of λ ($\lambda > 1$) time slots independently. Then the average number of active UEs in the considered time slot is $\frac{1}{\lambda} KN_c < KN_c$, and hence the uplink signals tend to be sparse (e.g., Figure 2 in [12]).

Note that bursty uplink traffic cannot be scheduled effectively in cellular systems due to the latency³ concerns. For instance, in LTE-A systems [13], the random access is commonly advocated [13]–[15] as an efficient protocol to accommodate a large number of machine-type communications with massive burst of low latency data. Denote the set of non-zero elements of \mathbf{x} as \mathcal{T} , i.e.,

$$\begin{cases} \mathbf{x}(i) \sim \mathcal{CN}(0, P_i), & i \in \mathcal{T} \\ \mathbf{x}(i) = 0, & i \notin \mathcal{T} \end{cases}, \quad (5)$$

where P_i is the transmit SNR of the user corresponding to $\mathbf{x}(i)$, $i \in \mathcal{T}$. Let $s \triangleq \#\mathcal{T} \ll KN_c$ and there are s

²For instance, the UEs send uplink reference signals regularly in TDD-LTE systems [23].

³To schedule uplink transmissions [13], the UE first sends a BW request through random access and the Node B then schedules the uplink resource. As such, uplink scheduling has significant protocol overhead and latency and it is not suitable to support massive UEs with small burst, low latency and long duty cycle requirement.

active⁴ UEs among \mathcal{U} in the considered time slot. Our target is to exploit the underlying sparsity in the uplink transmitted signals to reduce the fronthaul loading in C-RAN systems. The proposed scheme consists of *distributed compression* at the RRH as well as efficient *joint recovery* at the BBU pools. For robust implementation, the BBU pool in the C-RAN does not know the signal sparsity support \mathcal{T} (the set of active UEs) and the sparsity level $s \triangleq \#\mathcal{T}$ (the number of active UEs). We shall elaborate the distributed fronthaul compression scheme in the next section.

B. Distributed Fronthaul Compression in C-RAN Systems

In this section, we shall propose a distributed fronthaul compression scheme in C-RAN systems. As we can see in (3), the RRH can compress the received signals from the multi-access fading channel $\{\mathbf{y}_i : \forall i\}$ before sending them to the BBU pools for the joint recovery of \mathbf{x} . Suppose the i -th RRH uses a *local* compression matrix $\mathbf{A}_i \in \mathbb{C}^{R \times N_c}$ to compress the $(N_c \times 1)$ symbol vector \mathbf{y}_i into a lower dimensional $(R \times 1)$ signal vector \mathbf{z}_i ($R \leq N_c$) by

$$\mathbf{z}_i = \mathbf{A}_i \mathbf{y}_i. \quad (6)$$

Then the total number of measurements in $\{\mathbf{z}_i : \forall i\}$ to be transmitted to the BBU pools on the fronthaul is MR instead of MN_c . This represents a compression rate of $\alpha = \frac{R}{N_c} \leq 1$. Note that when $\alpha = 1$ (i.e., $R = N_c$), (6) is reduced to the scenario with no compression. On the other hand, the compression in (6) is a simple linear operation and hence it can be easily incorporated in the RRH of C-RAN systems.

Remark 1 (Consideration of Quantization in Fronthaul):

In this paper, the fronthaul compression is achieved by reducing the dimensions of the signal \mathbf{z}_i to be sent from the RRH to the BBU cloud. In practice, the absolute fronthaul loading (b/s) depends on both the *dimensions of \mathbf{z}_i* (i.e., R) and the *quantization*. The *dimension reduction of \mathbf{z}_i at the RRH* plays a first order role in fronthaul compression because a smaller signal dimension means a smaller number of complex numbers need to be quantized from the RRH to the BBU. For instance, from classical quantization theory [26], [27], to keep a constant distortion $\Delta \triangleq \frac{\|\mathbf{z}_i - \hat{\mathbf{z}}_i\|^2}{\|\mathbf{z}_i\|^2}$ (where $\hat{\mathbf{z}}_i$ denotes the quantized vector of \mathbf{z}_i), the required number of bits for quantization should scale linearly with the signal dimension R and is given by $B = \mathcal{O}(R \log \frac{1}{\Delta})$. As such, there is a genuine compression in (6) even when quantization effect is included.

Before we describe the distributed fronthaul compression scheme, we first give the generation method for the local compression matrix $\{\mathbf{A}_i\}$.

Definition 1 (Local Compression Matrices \mathbf{A}_i): The (r, c) -th entry of the $R \times N_c$ matrix \mathbf{A}_i is given by $\mathbf{A}_i(r, c) = \sqrt{\frac{1}{MR}} \exp(j\theta_{irc})$, where θ_{irc} is i.i.d. drawn from the uniform distribution over $[0, 2\pi)$.

Remark 2 (Interpretation of Definition 1): Note that \mathbf{A}_i serves as the *local measurement matrix* of \mathbf{y}_i , as in (6). In

⁴Here we call the (c, k) -th UE *active* if it is transmitting a signal, i.e., $x_k^{[c]}$ in (2) is non-zero.

the CS literature, it is shown that efficient and robust CS recovery can be achieved when the measurement matrix satisfies a proper RIP condition [21], and measurement matrices randomly generated from sub-Gaussian distribution [21] can satisfy the RIP with overwhelming⁵ probability [21]. As such, this randomized generation method has been widely used in the literature and we adopt this conventional approach to generate the local compression matrix $\{\mathbf{A}_i\}$ (as in Definition 1) with a good RIP. The factor $\sqrt{\frac{1}{MR}}$ in each entry in \mathbf{A}_i is for normalization. On the other hand, the compression matrices $\{\mathbf{A}_i\}$ are generated offline so that it is available at the BBU⁶.

The overall distributed fronthaul compression scheme in the C-RAN system can be described as follows (as illustrated in Figure 2):

Algorithm 1 (Distributed Fronthaul Compression)

- **Step 1 (Reception at RRHs):** The i -th RRH receives the channel outputs $\mathbf{y}_i = \mathbf{H}_i \mathbf{x} + \mathbf{n}_i$ as in (3).
- **Step 2 (Distributed Compression on the Fronthaul):** The i -th RRH compresses the received N_c -dimensional data vector \mathbf{y}_i into an R -dimensional vector \mathbf{z}_i with a local compression matrix $\mathbf{A}_i \in \mathbb{C}^{R \times N_c}$ by $\mathbf{z}_i = \mathbf{A}_i \mathbf{y}_i$, as in (6). The i -th RRH sends the compressed vector \mathbf{z}_i to the BBU pools on the fronthaul.
- **Step 3 (Centralized Signal Recovery at BBU Pools):** The BBU pools collect the compressed data symbols from all RRHs on the fronthaul, i.e., $\{\mathbf{z}_i : i = 1, 2, \dots, M\}$ and then jointly recover the transmitted signal $\{x_i^{[c]} : \forall i, c\}$ from the UEs. ■

Note that in Algorithm 1, the remaining question is how to conduct the signal recovery at the BBUs (Step 3) from the measurements $\{\mathbf{z}_i\}$ with reduced dimension (i.e., $MR \leq MN_c$). Different from classical distributed CS [19], [22], in which the objective is to recover the signal vectors that are compressed distributively (as illustrated in Figure 2(a)), our goal is to recover the transmitted signal \mathbf{x} from the UEs (as in Figure 2(b)). Existing results on the joint recovery of distributed CS [19], [22] cannot be applied, and we need to extend these results to incorporate the underlying multiaccess fading channels $\{H_{ik}^{[c]} : \forall i, k, c\}$ in C-RAN systems.

Challenge 1: End-to-end signal recovery of \mathbf{x} at the BBU from distributed CS measurements at the RRHs.

III. CS-ENABLED SIGNAL RECOVERY IN C-RAN SYSTEMS

In this section, we first elaborate the proposed signal recovery (i.e., step 3 in Algorithm 1), which exploits the signal sparsity and the structure of the multi-access fading channel to recover the transmitted signals $\{x_i^{[c]} : \forall i, c\}$ by the KN_c UEs. Based on that, we establish sufficient conditions on the required number of measurements at RRHs to achieve correct

⁵For an $R \times N$ matrix Φ i.i.d. generated from random sub-Gaussian distributions, it is shown that when $R = c_1 s \log N$, the probability that Φ fails to satisfy the s -th RIP with δ decays exponentially w.r.t. R as $\mathcal{O}(\exp(-c_2 R))$, where c_1 and c_2 are positive constants depending on δ [21].

⁶For instance, the compression matrices $\{\mathbf{A}_i\}$ can be initialized from the BBU and the distributed to the RRH during the setup of the C-RAN so that the BBU has the knowledge of $\{\mathbf{A}_i\}$

active user detection *with high probability* in the proposed algorithm. Note that based on the performance result of the correct active user detection, we shall further quantify the C-RAN capacity in Section IV.

A. End-to-End Sparse Signal Recovery Algorithm

The proposed signal recovery algorithm at the BBU pools consists of three major components: i) rough signal estimation of $\hat{\mathbf{x}}$ using CS techniques; ii) active user detection $\hat{\mathcal{T}}$ based on $\hat{\mathbf{x}}$; and iii) zero-forcing (ZF) receiver based on $\hat{\mathcal{T}}$. Figure 3 illustrates the block diagram of the signal recovery algorithm at the BBU pools. Note that the proposed recovery algorithm is different from the standard CS recovery in [20], [28], [29] because the proposed recovery algorithm has embraced the multi-access fading channel $\{H_{ik}^{[c]} : \forall i, k, c\}$ in the recovery process. The three components are elaborated in detail below.

- **Rough signal estimation of $\hat{\mathbf{x}}$ using CS techniques:**

We first formulate the rough signal estimation of $\hat{\mathbf{x}}$ into a standard CS problem. First, concatenate the compressed symbol vectors $\{\mathbf{z}_i \in \mathbb{C}^{R \times 1} : i = 1, 2, \dots, M\}$ into a long vector to be $\mathbf{z} = [\mathbf{z}_1^T \ \dots \ \mathbf{z}_M^T]^T \in \mathbb{C}^{MR \times 1}$. Then, (3) can be equivalently written as

$$\mathbf{z} = \Theta \mathbf{x} + \mathbf{n}, \quad (7)$$

where \mathbf{n} is the aggregate measurement noise

$$\mathbf{n} = [(\mathbf{A}_1 \mathbf{n}_1)^T \ \dots \ (\mathbf{A}_M \mathbf{n}_M)^T]^T \in \mathbb{C}^{MR \times 1}, \quad (8)$$

and Θ is given by (a detailed expression of Θ is also given in (12))

$$\Theta = [(\mathbf{A}_1 \mathbf{H}_1)^T \ \dots \ (\mathbf{A}_M \mathbf{H}_M)^T]^T \in \mathbb{C}^{MR \times KN_c}. \quad (9)$$

Therefore, (7) matches the standard CS model in which \mathbf{z} is the measurements, Θ is the aggregate *measurement matrix*, \mathbf{x} is the sparse signal vector to be recovered and \mathbf{n} is the CS measurement noise (with $\mathbb{E}(\|\mathbf{n}\|^2) = N_c$). Note that knowledge of Θ can be available at the BBU from (9) and the fact that both $\{\mathbf{H}_i\}$ and $\{\mathbf{A}_i\}$ are available at the BBU. Since the above formulation (7) has incorporated the channel fading of $\{H_{ik}^{[c]}\}$ into the CS measurement model, it enables us to conduct the end-to-end recovery of \mathbf{x} . Using the classical basis⁷ pursuit (BP) [20] CS recovery technique, the rough signal recovery of $\hat{\mathbf{x}}$ can be formulated as

$$\mathcal{P}_1 : \quad \min_{\hat{\mathbf{x}}} \quad \|\hat{\mathbf{x}}\|_1 \\ \text{s.t.} \quad \|\Theta \hat{\mathbf{x}} - \mathbf{z}\| \leq \lambda. \quad (10)$$

where λ is a proper threshold parameter.

- **Active user detection $\hat{\mathcal{T}}$ based on $\hat{\mathbf{x}}$:** The following criterion is proposed to detect the set of active UEs $\hat{\mathcal{T}}$:

$$\hat{\mathcal{T}} = \arg \min_{\hat{\mathcal{T}}} \#\hat{\mathcal{T}}, \quad (11) \\ \text{s.t.} \quad \begin{cases} |\hat{\mathbf{x}}(i)| \geq |\hat{\mathbf{x}}(j)|, \forall i \in \hat{\mathcal{T}}, \quad j \notin \hat{\mathcal{T}}, \\ \left\| \left(\mathbf{I} - \Theta_{\hat{\mathcal{T}}} \Theta_{\hat{\mathcal{T}}}^\dagger \right) \mathbf{z} \right\| \leq \lambda \text{ OR } \#\hat{\mathcal{T}} = MR. \end{cases}$$

⁷Among various CS recovery algorithms [20], [28]–[30] (including BP [20], OMP [28], CoSaMP [29] and SP [30]), the BP is shown to have competitive theoretical as well as empirical recovery performance [20], and it does not require the knowledge of the sparsity level (i.e., $\#\mathcal{T}$). Therefore, in this paper, we adopt the BP approach to conduct the rough estimation of $\hat{\mathbf{x}}$ in Step 1.

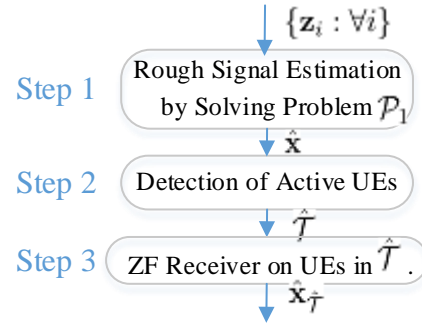


Figure 3. Illustration of the three major steps in signal recovery at the BBU pools (Algorithm 2).

where $\Theta_{\hat{\mathcal{T}}}^\dagger \triangleq (\Theta_{\hat{\mathcal{T}}}^H \Theta_{\hat{\mathcal{T}}})^{-1} \Theta_{\hat{\mathcal{T}}}^H$ denotes the Moore-Penrose pseudoinverse of $\Theta_{\hat{\mathcal{T}}}$.

- **Zero-forcing (ZF) receiver based on $\hat{\mathcal{T}}$:** The BBU pools apply the zero-forcing receiver $\mathbf{U} = (\Theta_{\hat{\mathcal{T}}}^\dagger)^H$ [31] to recover the transmitted signals from the UEs in $\hat{\mathcal{T}}$, i.e., $\hat{\mathbf{x}}_{\hat{\mathcal{T}}} = \Theta_{\hat{\mathcal{T}}}^\dagger \mathbf{z}$, $\hat{\mathbf{x}}_{\{1, \dots, KN_c\} \setminus \hat{\mathcal{T}}} = \mathbf{0}$.

The overall signal recovery at the BBU pools is summarized in Algorithm 2 (as well as in Figure 3).

Algorithm 2 (Joint Signal Recovery in Uplink C-RAN Systems with CS Techniques)

- **Step 1 (Rough Signal Estimation Using BP):** Solve Problem \mathcal{P}_1 to obtain $\hat{\mathbf{x}}$.

- **Step 2 (Active User Detection):** Find the solution $\hat{\mathcal{T}}$ to (11) via the following steps: First sort $\{|\hat{\mathbf{x}}(i)| : i = 1, \dots, KN_c\}$ in descending order to obtain the sorted indices $\{i_1, i_2, \dots, i_{KN_c}\}$, initialize $k = 1$ and $\hat{\mathcal{T}} = \{i_1\}$ and then execute the following to find $\hat{\mathcal{T}}$.

- *(Greedy Detection):* If $\left\| \left(\mathbf{I} - \Theta_{\hat{\mathcal{T}}} \Theta_{\hat{\mathcal{T}}}^\dagger \right) \mathbf{z} \right\| \leq \lambda$ or $k = MR$, then stop and output $\hat{\mathcal{T}}$. Else, update $k = k + 1$, $\hat{\mathcal{T}} = \hat{\mathcal{T}} \cup \{i_k\}$ and repeat.

- **Step 3 (Zero-forcing Receiver):** Based on the estimated set of UEs $\hat{\mathcal{T}}$, apply the linear zero-forcing receiver $\mathbf{U} = (\Theta_{\hat{\mathcal{T}}}^\dagger)^H$ [31] to recover the transmitted signals from the UEs in $\hat{\mathcal{T}}$, i.e., $\hat{\mathbf{x}}_{\hat{\mathcal{T}}} = (\Theta_{\hat{\mathcal{T}}}^\dagger) \mathbf{z}$, $\hat{\mathbf{x}}_{\{1, \dots, KN_c\} \setminus \hat{\mathcal{T}}} = \mathbf{0}$.

Remark 3 (Implementation Consideration of Algorithm 2): Note that the computation of Algorithm 2 is dominated by solving the l_1 -norm minimization (Problem \mathcal{P}_1), which can be accomplished with a complexity of $O((KN_c)^3)$ [21]. On the other hand, Algorithm 2 does not require knowledge of the sparsity level $\#\mathcal{T}$ (i.e., the number of active UEs) because this can be automatically detected in Step 2 of Algorithm 2. Finally, in Step 3 of Algorithm 2, the classical ZF receiver is adopted because of its simplicity and asymptotical optimality in high SNR regions [31]. ■

B. Analysis of Correct Active User Detection in Algorithm 2

Note that when the detected set of active UEs in Algorithm 2 is correct, i.e., $\hat{\mathcal{T}} = \mathcal{T}$, Step 3 in Algorithm 2 will be *reduced to classical ZF* on the set of the active uplink UEs \mathcal{T} directly.

⁸Note that we have constrained the maximum size of $\hat{\mathcal{T}}$ to be MR as in (11). This is because we have a total of MR observations at the BBU so that we can recover MR unknowns at most.

$$\Theta = \begin{bmatrix} \begin{bmatrix} H_{11}^{[1]} \mathbf{A}_1(1,1) & \cdots & H_{1K}^{[1]} \mathbf{A}_1(1,1) \\ \vdots & \ddots & \vdots \\ H_{11}^{[1]} \mathbf{A}_1(R,1) & \cdots & H_{1K}^{[1]} \mathbf{A}_1(R,1) \end{bmatrix} & \cdots & \begin{bmatrix} H_{11}^{[N_c]} \mathbf{A}_1(1,N_c) & \cdots & H_{1K}^{[N_c]} \mathbf{A}_1(1,N_c) \\ \vdots & \ddots & \vdots \\ H_{11}^{[N_c]} \mathbf{A}_1(R,N_c) & \cdots & H_{1K}^{[N_c]} \mathbf{A}_1(R,N_c) \end{bmatrix} \\ \vdots & \ddots & \vdots \\ \begin{bmatrix} H_{M1}^{[1]} \mathbf{A}_M(1,1) & \cdots & H_{MK}^{[1]} \mathbf{A}_M(1,1) \\ \vdots & \ddots & \vdots \\ H_{M1}^{[1]} \mathbf{A}_M(R,1) & \cdots & H_{MK}^{[1]} \mathbf{A}_M(R,1) \end{bmatrix} & \cdots & \begin{bmatrix} H_{M1}^{[N_c]} \mathbf{A}_M(1,N_c) & \cdots & H_{MK}^{[N_c]} \mathbf{A}_M(1,N_c) \\ \vdots & \ddots & \vdots \\ H_{M1}^{[N_c]} \mathbf{A}_M(R,N_c) & \cdots & H_{MK}^{[N_c]} \mathbf{A}_M(R,N_c) \end{bmatrix} \end{bmatrix} \quad (12)$$

This is the desired performance and it is also asymptotically optimal because of the asymptotical optimality of ZF in high SNR [31]. Under correct active user detection, further analysis [31] on ZF can also be conducted to give further characterization of the C-RAN communication performance (e.g., sum capacity, which will be discussed in Section IV). Therefore, it is critical to first understand the performance of active user detection in Algorithm 2.

Challenge 2: Analyze the probability of correct active user detection, i.e., $\hat{\mathcal{T}} = \mathcal{T}$ in Algorithm 2.

In Algorithm 2, the rough estimation of $\hat{\mathbf{x}}$ in **Step 1** plays an important role in the detection of active user $\hat{\mathcal{T}}$ in **Step 2**. As such, we shall first characterize Step 1 in Algorithm 2 (the BP in Problem \mathcal{P}_1). In the literature, RIP [20] is commonly adopted to facilitate the performance analysis of the BP. We first review the notion of the RIP in Definition 2 and the associated performance result of BP under RIP in Lemma 1.

Definition 2 (Restricted Isometry Property [20]): Matrix $\Theta \in \mathbb{C}^{MR \times KN_c}$ satisfies a k -th order RIP with a prescribed *restricted isometry constant* (RIC) δ if $0 \leq \delta < 1$ and

$$(1 - \delta) \|\mathbf{x}\|^2 \leq \|\Theta \mathbf{x}\|^2 \leq (1 + \delta) \|\mathbf{x}\|^2$$

holds for all $\mathbf{x} \in \mathbb{C}^{KN_c \times 1}$ where $\|\mathbf{x}\|_0 \leq k$. ■

Denote event $\mathcal{E}_{k,\delta}$ as follows:

$$\mathcal{E}_{k,\delta} : \quad \Theta \text{ satisfies a } k\text{-th order RIP with RIC } \delta. \quad (13)$$

From [20], we have the following lemma on the recovery performance regarding problem \mathcal{P}_1 .

Lemma 1 (Robust Recovery of BP under RIP [21]):

Suppose the threshold parameter λ in \mathcal{P}_1 satisfies $\lambda \geq \|\mathbf{n}\|_F$. If event $\mathcal{E}_{2s,\delta}$ happens, where $s \triangleq \#\mathcal{T} \ll KN_c$, and the RIC δ satisfies $\delta < \sqrt{2} - 1$, then the solution $\hat{\mathbf{x}}$ to \mathcal{P}_1 satisfies

$$\|\mathbf{x} - \hat{\mathbf{x}}\| \leq c_2 \lambda, \quad (14)$$

where $c_1 = \frac{\lambda^2 - N_c}{4N_c}$ and $c_2 = 4 \frac{\sqrt{1+\delta}}{1-(1+\sqrt{2})\delta}$. ■

Based on Lemma 1, we obtain the following *conditions* for correct active user detection and the associated performance result in Algorithm 2.

Theorem 1 (Correct Active User Detection Conditions):

Suppose $\lambda \geq \|\mathbf{n}\|_F$ and event $\mathcal{E}_{2s,\delta}$ happens where $\delta < \sqrt{2} - 1$. If event \mathcal{E}_1 is true where

$$\mathcal{E}_1 : |\mathbf{x}(i)| > \sqrt{2} c_2 \lambda, \quad \forall i \in \mathcal{T},$$

c_2 is in Lemma 1, then

1) the detected $\hat{\mathcal{T}}$ in Step 2 of Algorithm 2 is correct, i.e., $\hat{\mathcal{T}} = \mathcal{T}$.

2) the recovered signal $\hat{\mathbf{x}}$ from Step 3 of Algorithm 2 satisfies $\|\mathbf{x} - \hat{\mathbf{x}}\| \leq \frac{1}{\sqrt{1-\delta}} \|\mathbf{n}\|$.

Proof: See Appendix A. ■

Remark 4 (Fronthaul Quantization): The results of Theorem 1 also cover the case with quantization in the fronthaul as well. Suppose that the signal \mathbf{z} is further *quantized* with b quantization bits per dimension. The quantized $\hat{\mathbf{z}}$ is given by $\hat{\mathbf{z}} = \mathbf{z} + \hat{\mathbf{n}}$, where $\hat{\mathbf{n}}$ is the quantization noise ($\|\hat{\mathbf{n}}\|$ scales in the order of $\mathcal{O}(2^{-\frac{b}{2}}) \|\mathbf{z}\| \sim \mathcal{O}(2^{-\frac{b}{2}} \sqrt{\sum_{i \in \mathcal{T}} P_i})$ [26], [27]). Then the aggregate signal model becomes $\hat{\mathbf{z}} = \mathbf{z} + \hat{\mathbf{n}} = \Theta \mathbf{x} + \mathbf{n} + \hat{\mathbf{n}}$, where $(\mathbf{n} + \hat{\mathbf{n}})$ replaces the role of \mathbf{n} in (7) with $\|\hat{\mathbf{n}} + \mathbf{n}\| \leq \|\hat{\mathbf{n}}\| + \|\mathbf{n}\| \sim \mathcal{O}(2^{-\frac{b}{2}} \sqrt{\sum_{i \in \mathcal{T}} P_i}) + \|\mathbf{n}\|$. From Theorem 1, $\hat{\mathcal{T}} = \mathcal{T}$ can still be achieved in Step 2 and the final recovered signal $\hat{\mathbf{x}}$ in Step 3 satisfies $\|\mathbf{x} - \hat{\mathbf{x}}\| \leq \frac{1}{\sqrt{1-\delta}} \|\hat{\mathbf{n}} + \mathbf{n}\|$ in Algorithm 2.

Note that classical BP CS recovery (e.g., Problem \mathcal{P}_1) requires that the measurement noise is bounded (e.g., $\|\mathbf{n}\|_F \leq \lambda$ as in Lemma 1) [21]. However, due to the Gaussian factors in the noise (i.e., $\{\mathbf{n}_i : \forall i\}$ in (8)), the aggregate noise $\|\mathbf{n}\|_F$ may not always be bounded. By using the tools from concentration inequalities [32], we first show below that $\|\mathbf{n}\|_F$ can be bounded *with high probability*, despite the complicated form of the colored noise \mathbf{n} in (8).

Lemma 2 (Bounded Noise with High Probability):

Suppose $\lambda \geq \sqrt{2N_c}$. The probability that $\|\mathbf{n}\|_F \leq \lambda$ happens is at least $1 - \exp(-c_1 M)$, where $c_1 = \frac{\lambda^2 - N_c}{4N_c}$.

Proof: See Appendix B. ■

From Theorem 1 and Lemma 2, we further obtain the following lower bound on the probability of correct active user detection.

Theorem 2 (Probability of Correct Active User Detection):

The probability of correct active UEs $\hat{\mathcal{T}}$ detection, i.e., $\hat{\mathcal{T}} = \mathcal{T}$, in Step 2 of Algorithm 2 satisfies

$$\Pr(\hat{\mathcal{T}} = \mathcal{T}) \geq \Pr(\mathcal{E}_{2s,\delta}) \times \left(1 - \exp(-c_1 M) - s \cdot \left(1 - \exp\left(-\frac{2(c_2 \lambda)^2}{P_{\min}}\right) \right) \right) \quad (15)$$

where $P_{\min} \triangleq \min_{i \in \mathcal{T}} P_i$, $c_1 = \frac{\lambda^2 - N_c}{4N_c}$, c_2 is in Lemma 1 and $\Pr(\mathcal{E}_{2s,\delta})$ denotes the probability that event $\mathcal{E}_{k,\delta}$ in (13) happens with parameters $k = 2s$ and $\delta < \sqrt{2} - 1$.

Proof: See Appendix C. ■

Note that the result of correct active user detection in Theorem 2 is important for further characterization of the uplink C-RAN capacity (Theorem 4 in Section IV). From (15), in high SNR regimes, i.e., $P_{\min} \triangleq \min_{i \in \mathcal{T}} P_i \gg 4c_2^2 N_c$, with λ

in Problem \mathcal{P}_1 being adaptive to P_{\min} (e.g., $\lambda = \left(\frac{P_{\min} N_c}{4c_2^2}\right)^{\frac{1}{4}}$), the factor after $\Pr(\mathcal{E}_{2s,\delta})$ in (15) approaches 1, and hence (15) is simplified to be $\Pr(\hat{\mathcal{T}} = \mathcal{T}) \gtrsim \Pr(\mathcal{E}_{2s,\delta})$. Consequently, the probability of $\hat{\mathcal{T}} = \mathcal{T}$ can be lower bounded by the probability of event $\mathcal{E}_{2s,\delta}$ only. This relationship under high SNR simplifies the analysis and potentially leads to elegant results. Note that in (15), it remains unknown what $\Pr(\mathcal{E}_{2s,\delta})$ is. A more fundamental question is whether $\mathcal{E}_{2s,\delta}$ can happen or not (i.e., whether the RIP condition can hold for Θ). We shall investigate this issue in the next section.

C. Characterization of the RIP for Θ

In this section, we justify that the RIP condition can be satisfied for our aggregate measurement matrix Θ (i.e., $\mathcal{E}_{2s,\delta}$ can happen). Note that not all matrices can satisfy the RIP condition and justifying the RIP of a random matrix is also highly challenging in general [21]. For instance, to prove the RIP property for conventional *i.i.d.* sub-Gaussian random matrices, the tools of concentration inequalities are needed and lots of math derivations are usually involved to characterize the tail probabilities of sub-Gaussian vectors [33]. On the other hand, the characterization of the RIP for the random matrix Θ in (12) will be *more* complicated as Θ contains a very complicated *structure*. Specifically, the randomness of Θ comes from both the block diagonal fading matrices $\{\mathbf{H}_i\}$ and the distributed compression matrices $\{\mathbf{A}_i\}$. From the expression of Θ in (12), we have the following two observations:

- **Observation I:** The columns of Θ are *correlated* due to the shared random factors of $\{\mathbf{A}_i(r, c)\}$.
- **Observation II:** The rows of Θ are *correlated* due to the shared random factors of $\{\mathbf{H}_i\}$.

As such, conventional techniques [33] for characterizing the RIP for *i.i.d.* sub-Gaussian random matrices cannot be applied to our scenario. In the literature, there are a few works of RIP characterization on structured measurement matrices, such as the Random Demodulator matrix in [34], the Toeplitz matrix in [35], and the random Gaussian matrix with *i.i.d.* row vectors while having correlated entries within each row [36]. However, these works [34]–[36] cannot be used in our scenario due to the different structure of Θ as described above.

Challenge 3: Analyze the RIP of Θ despite the complicated structures in the random matrix Θ in (12).

In the following, we shall establish the RIP condition for Θ . Despite of the complicated structures above, one important feature of Θ is that under a given realization of $\{\mathbf{H}_i\}$, different *columns* of Θ are *conditionally independent*. On the other hand, R. Vershynin et al. shows in [37] that random sub-Gaussian matrices with *independent columns* is likely to satisfy the RIP with high probability under certain mild conditions. This result [37] enables us to first deploy the conditional probability theory to *decompose* the proof of RIP of Θ into several concentration inequalities. We then manage to prove each of these concentration inequalities by following the derivation techniques in [34] and [37]. Specifically, we

show that when the number of measurements R at each RRH scales in the order of $\mathcal{O}\left(\frac{s \log^6 KN_c}{M}\right)$, the aggregate measurement matrix Θ (with special structures) can satisfy the RIP with high probability.

Theorem 3 (RIP of Θ): Suppose $KN_c \geq M \geq C_1 k_0 \log\left(\frac{eK}{k_0}\right) \log^2(KN_c)$, $k_0 = \min(K, k)$. If the number of measurements R at each RRH satisfies $R \geq \frac{C_2 \delta^{-2k} \log^6 KN_c}{M}$, then

$$\Pr(\mathcal{E}_{k,\delta}) \geq 1 - \frac{4}{KN_c}, \quad (16)$$

where $\mathcal{E}_{k,\delta}$ is in (13) with parameters k and δ , C_1 and C_2 are constants that depend on δ and \bar{g} in Assumption 1, and are given in Appendix D.

Proof: See Appendix D. ■

Remark 5 (Insights from Theorem 3): Note that Theorem 3 gives a *sufficient* condition on the number of measurements at the RRHs to satisfy the RIP with high probability. Combining the result in Theorem 3 with Theorem 2, we derive that in high SNR regimes (i.e., $\min_{i \in \mathcal{T}} P_i \gg 4c_2^2 N_c$), when the number of measurements R at each RRH scales in the order⁹ of $\mathcal{O}\left(\frac{s \log^6 KN_c}{M}\right)$, it suffices to achieve a high probability of correct active user detection $\hat{\mathcal{T}} = \mathcal{T}$ (i.e., $\Pr(\hat{\mathcal{T}} = \mathcal{T}) \gtrsim 1 - \frac{4}{KN_c}$). Based on the established RIP condition in Theorem 3, we shall further obtain a lower bound on the C-RAN performance in Section IV. We point out that the established RIP in Theorem 3 in fact justifies the *feasibility* of applying CS to achieve distributed fronthaul compression in C-RAN with exploitation of the uplink user sparsity.

Remark 6 (Significance of the RIP for System Design):

Note that in the CS literature, the RIP plays a *central* role in characterizing the CS recovery performance. For instance, provided that the CS measurement matrix satisfies certain RIP condition, these state-of-the-art CS recovery algorithms, including BP [20], CoSaMP [29] and SP [30], are all shown to achieve certain performance guarantees. Unfortunately, establishing technical conditions for RIP is highly non-trivial and depends very much on the structure of the measurement matrix in the compressive sensing problems. In our case, the existing techniques for proving RIP is not applicable due to the special structure of the measurement matrix. The proposed new proving technique in Theorem 3 can also be used to establish RIP of other C-RAN applications.

IV. TRADEOFF ANALYSIS BETWEEN UPLINK CAPACITY AND FRONTHAUL LOADING IN THE C-RAN

In this section, we shall quantify the average uplink capacity of the proposed distributed compression and joint recovery scheme in the C-RAN. From the results, we derive simple

⁹Note that in the RIP result in (16), there is an increase in the required number of measurements compared with the conventional result on random matrices with *i.i.d.* sub-Gaussian entries (i.e., from $\mathcal{O}(s \log KN_c)$ to $\mathcal{O}(s \log^6 KN_c)$). This penalty might be due to the special measurement structure in C-RAN systems (as in Observation I-II). However, the high order of 6 on the logarithmic factors might not be necessary and it is probably parasitic as a consequence of the techniques used to derive the theorem (similar to [34]). The empirical tests in Section V show that a moderate number of measurements at each RRH already leads to a good signal recovery performance.

tradeoff results between the uplink communication performance and the fronthaul loading in C-RAN systems.

Challenge 4: Analyze the tradeoff relationship between the C-RAN performance and the fronthaul loading.

Suppose the transmit SNR of the active users are the same, i.e., $P_i = P, \forall i \in \mathcal{T}$ for simple results. With a ZF receiver, as in Step 3 of Algorithm 2, the recovered signal $\hat{\mathbf{x}}_{\hat{\mathcal{T}}}$ from the set of UEs $\hat{\mathcal{T}}$ can be expressed by

$$\hat{\mathbf{x}}_{\hat{\mathcal{T}}} = (\Theta_{\hat{\mathcal{T}}})^\dagger \mathbf{z} = \mathbf{x}_{\hat{\mathcal{T}}} + \underbrace{(\Theta_{\hat{\mathcal{T}}})^\dagger \Theta_{\mathcal{T} \setminus \hat{\mathcal{T}}} \mathbf{x}_{\mathcal{T} \setminus \hat{\mathcal{T}}}}_{(a)} + \underbrace{(\Theta_{\hat{\mathcal{T}}})^\dagger \mathbf{n}}_{(b)}, \quad (17)$$

where (a) can be regarded as the interference brought by the detection error of the active UEs and (b) is the aggregate noise. Based on (17), the sum capacity R_{sum} [31] with the ZF receiver, is

$$R_{sum} = \sum_{l=1}^{\#\hat{\mathcal{T}}} \log \left(1 + \frac{P_l}{\alpha_l} \right), \quad (18)$$

where $P_l = P$ if the l -th element of $\hat{\mathcal{T}}$ belongs to \mathcal{T} and $P_l = 0$ otherwise, and α_l is the l -th diagonal element of the interference plus noise covariance matrix Ψ ,

$$\Psi = \Theta_{\hat{\mathcal{T}}}^\dagger \left(P \Theta_{\mathcal{T} \setminus \hat{\mathcal{T}}} \Theta_{\mathcal{T} \setminus \hat{\mathcal{T}}}^H + \mathbf{A} \mathbf{A}^H \right) (\Theta_{\hat{\mathcal{T}}})^H, \quad (19)$$

where $\mathbf{A} = \text{diag}([\mathbf{A}_1 \ \cdots \ \mathbf{A}_M])$ and $\mathbf{A} \mathbf{A}^H$ is the covariance matrix of the colored noise \mathbf{n} in (8). Note that when the information of the active UEs is correct, i.e., $\hat{\mathcal{T}} = \mathcal{T}$, we obtain $P_l = P, \forall l = 1, \dots, \#\hat{\mathcal{T}}$ and Ψ in (19) can be reduced to

$$\Psi = (\Theta_{\hat{\mathcal{T}}})^\dagger (\mathbf{A} \mathbf{A}^H) (\Theta_{\hat{\mathcal{T}}})^H. \quad (20)$$

Based on (18)-(20) and by using the probability results regarding correct active user detection in Theorem 2, we obtain the following bound on the *average* uplink capacity $\mathbb{E}(R_{sum})$ of C-RAN systems (with respect to the randomness of the multiaccess channel $\{H_{ik}^{[c]} : \forall i, k, c\}$ and the local compression matrices $\{\mathbf{A}_i : \forall i\}$).

Theorem 4 (Bound of Average C-RAN Capacity): Denote the compression rate at the RRHs as α , i.e., $\alpha \triangleq \frac{R}{N_c}$. The average capacity $\mathbb{E}(R_{sum})$ satisfies the following bound:

- **Upper Bound:** $\mathbb{E}(R_{sum}) \leq s \log(1 + M\alpha P)$.
- **Lower Bound:** Under high SNR condition, i.e., $P \gg 4c_2^2 N_c$ and supposing the parameter λ in Problem \mathcal{P}_1 is given by $\lambda = \left(\frac{PN_c}{4c_2^2}\right)^{\frac{1}{4}}$, $\mathbb{E}(R_{sum})$ satisfies

$$\mathbb{E}(R_{sum}) \geq \Pr(\mathcal{E}_{2s,\delta}) \cdot s \log(1 + (1 - \delta)M\alpha P), \quad (21)$$

where $\Pr(\mathcal{E}_{2s,\delta})$ denotes the probability that event $\mathcal{E}_{2s,\delta}$ in (13) happens with parameters $k = 2s$ and $\delta < \sqrt{2} - 1$.

Proof: See Appendix G. ■

From Theorem 3 and 4, we further have the following Corollary.

Corollary 1 (Tradeoff Results): Consider a high SNR scenario, i.e., $P \gg 4c_2^2 N_c$ and suppose $KN_c \geq M \geq C_1 k_0 \log\left(\frac{eK}{k_0}\right) \log^2(KN_c)$, where $k_0 = \min(K, 2s)$ and λ in Problem \mathcal{P}_1 is given by $\lambda = \left(\frac{PN_c}{4c_2^2}\right)^{\frac{1}{4}}$ and. If the compression

ratio $\alpha \triangleq \frac{R}{N_c}$ at each RRH satisfies $\alpha \geq \frac{2C_2\delta^{-2}s \log^6 KN_c}{MN_c}$ with $\delta < \sqrt{2} - 1$, then the average sum capacity $\mathbb{E}(R_{sum})$ satisfies

$$\left(1 - \frac{4}{KN_c}\right) s \log(1 + M(1 - \delta)\alpha P) \leq \mathbb{E}(R_{sum}) \leq s \log(1 + M\alpha P) \quad (22)$$

where c_2 is in Lemma 1, and C_1 and C_2 are in Theorem 3.

Proof: (Sketch) The upper bound follows directly from Theorem 4 and the lower bound is obtained by substituting $\Pr(\mathcal{E}_{2s,\delta}) \geq 1 - \frac{4}{KN_c}$ in Theorem 3 into (21). ■

Remark 7 (Interpretation of Corollary 1): Note that Corollary 1 gives a closed-form lower/upper bounds on the average throughput $\mathbb{E}(R_{sum})$ under certain requirements of the compression ratio α . From (22), both the lower bound and upper bound of the average capacity are in the order of $\mathcal{O}(s \log(M\alpha P))$. Therefore, when the compression ratio $\alpha \triangleq \frac{R}{N_c}$ at each RRH satisfies the order of $\mathcal{O}\left(\frac{s \log^6 KN_c}{MN_c}\right)$, it is sufficient to achieve a sum throughput of $\mathcal{O}(s \log(M\alpha P))$ in the uplink C-RAN. Furthermore, from (22), we observe that the distributed fronthaul compression α causes a capacity loss in terms of receiving SNR reduction with a factor of the compression rate α on the fronthaul. This result uncovers the simple tradeoff relationship between the communication performance and the fronthaul loading in the uplink C-RAN.

V. NUMERICAL RESULTS

In this section, we verify the effectiveness of the proposed signal recovery and distributed fronthaul compression scheme via simulations. Specifically, the following baselines will be considered for performance benchmarks:

- **Baseline 1 (MMSE Receiver [31]):** The BBUs jointly recover the transmitted signal \mathbf{x} using conventional MMSE Multi-user Detection [31].
- **Baseline 2 (Separate MMSE Receiver):** Each UE is associated with the RRH with the largest large-scale fading gain. Each RRH *separately* recovers the transmitted signal for the set of the associated UEs using MMSE Multi-user Detection [31].
- **Baseline 3 (OMP-based ZF [28]):** Instead of using a convex relaxation approach, as in Algorithm 2, the BBU pools choose to detect the set of active UEs using the OMP [28], and then apply the ZF receiver to recover the transmitted signals.
- **Baseline 4 (Genie-Aided ZF):** The set of active UEs \mathcal{T} is *known* at the BBU pools so that the BBU pools directly apply ZF on the set of active UEs \mathcal{T} . Note that this serves as a performance upper on the proposed scheme.

Consider a C-RAN system with $M = 40$ single-antenna RRHs and a total of $KN_c = 640$ single-antenna mobile UEs being served on $N_c = 32$ subcarriers (i.e., each subcarrier is allocated to $K = 20$ UEs). Suppose the RRHs and the mobile UEs are randomly and evenly distributed in the circular region with radius 2km. The path loss between the UEs and distributed RRHs are generated using the standard Log-distance path loss model, with path loss exponent 2.5. Denote the number of active UEs as s , the number of measurements

at each RRH as R , and the transmit SNR at the active UEs as P . The threshold parameter λ in Algorithm 2 is set as $\lambda = \sqrt{2N_c}$. We further consider that the transmitted signals on the fronthaul are quantized with $b = 10$ quantization bits per dimension ($b = 10$ for each complex number).

A. Throughput Versus Compression Rate

Figure 4 illustrates the *per active-user* throughput (i.e., $\frac{1}{s}\mathbb{E}(R_{sum})$) of the C-RAN versus the fronthaul loading (in terms of quantization bits per fronthaul link) under the number of active UEs $s = 64$ and transmit SNR $P = 20$ dB. From this figure, we observe that the throughput gets larger as the fronthaul loading increases. In addition, the proposed scheme approaches the performance of the Genie-aided ZF as the fronthaul loading increases. This is because as fronthaul loading (measurements on the fronthaul) gets larger, the probability of satisfying the RIP gets larger and the probability of correct active user detection also gets larger. Consequently, the proposed scheme would approach the Genie-aided ZF.

B. Throughput Versus Transmit SNR

Figure 5 further illustrates the *per active-user* throughput of the C-RAN system versus the transmit SNR P under number of active UEs $s = 64$ and per fronthaul bits $B = 60$. From this figure, we observe that the throughput of the proposed scheme gets larger as the transmit SNR increases, and it performs the same as the Genie-aided ZF in the high SNR regimes. This is because the probability of correct detection of the active UEs gets larger as SNR increases, as indicated in Theorem 2. Note that the proposed upper bound in Thm. 4 can still act as a performance upper bound in cases of fronthaul quantization as quantization would lead to performance degradations.

C. Throughput Versus Number of Active UEs

Figure 6 further illustrates the *per active-user* throughput of the C-RAN system versus the number of active UEs under transmit SNR $P = 20$ dB and per fronthaul bits $B = 60$. From this figure, we observe that the proposed scheme achieves the same performance as the Genie-aided ZF in the regime with a small number of active UEs. This is because nearly perfect detection of the active UEs is achieved in small sparsity regimes. This comparison further highlights the importance of correct active user detection in C-RAN systems.

VI. CONCLUSION

In this paper, we apply CS techniques to uplink C-RAN systems to achieve distributed fronthaul compression with exploitation of UE signal sparsity. We incorporate multi-access fading in C-RAN system into the CS formulation and we conduct an end-to-end recovery of the transmitted signals from the users. We show that the aggregate measurement matrix in the C-RAN, which contains both the distributed compression and multiaccess fading, can still satisfy the *restricted isometry property* with high probability. This result provides the foundation to apply CS to the uplink C-RAN systems. Based on this, we further analyze the probability of correct active

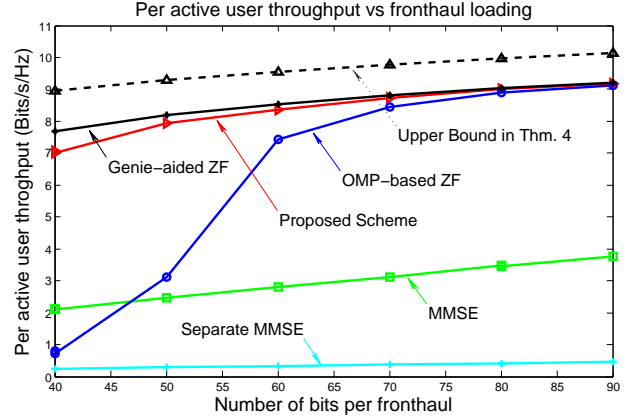


Figure 4. Throughput versus the per fronthaul loading in terms of the number of bits B under transmit SNR $P = 20$ dB and number of active UEs $s = 64$.

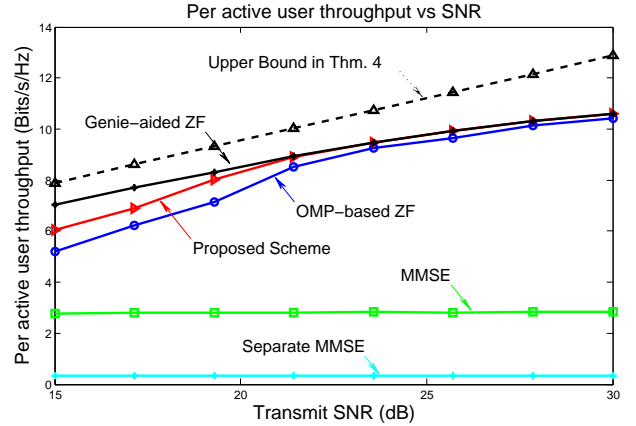


Figure 5. Throughput versus the transmit SNR P under per fronthaul quantization bits $B = 60$ and number of active UEs $s = 64$.

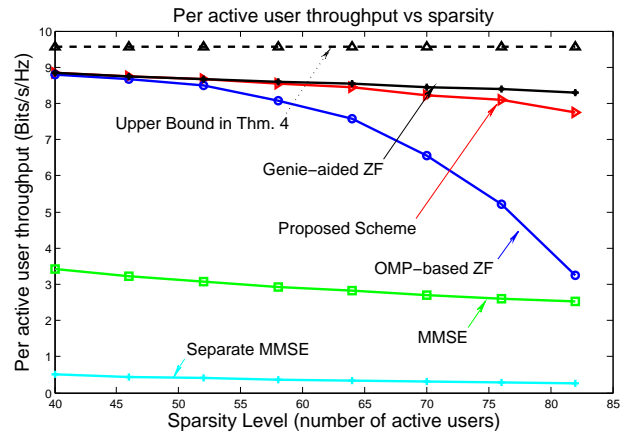


Figure 6. Throughput versus the number of active UEs s under per fronthaul quantization bits $B = 60$ and transmit SNR $P = 20$ dB.

user detection and quantify the tradeoff relationship between the uplink capacity and the distributed fronthaul loading in C-RAN.

APPENDIX

A. Proof of Theorem 1

We first prove the first item in Theorem 1. i) First, the s indices in \mathcal{T} must be arranged at the front in the sorted indices $\{i_1, \dots, i_{KN_c}\}$ in Step 2 of Algorithm 2. Otherwise, i.e., there exists a $i \in \mathcal{T}$, $j \notin \mathcal{T}$ where $|\hat{\mathbf{x}}(j)| \geq |\hat{\mathbf{x}}(i)|$, we would obtain

$$\|\mathbf{x} - \hat{\mathbf{x}}\| \geq \sqrt{|\mathbf{x}(i) - \hat{\mathbf{x}}(i)|^2 + |0 - \hat{\mathbf{x}}(j)|^2} \geq \frac{1}{\sqrt{2}}|\mathbf{x}(i)| > c_2\lambda$$

which contradicts (14). ii) Second, the greedy selection of $\hat{\mathcal{T}}$ cannot stop with $\#\hat{\mathcal{T}} < s$. Otherwise, i.e., there must exist an $i \in \mathcal{T}$ and $i \notin \hat{\mathcal{T}}$. we obtain

$$\begin{aligned} \left\| (\mathbf{I} - \Theta_{\hat{\mathcal{T}}} \Theta_{\hat{\mathcal{T}}}^\dagger) \mathbf{z} \right\|_F &\geq \left\| (\mathbf{I} - \Theta_{\hat{\mathcal{T}}} \Theta_{\hat{\mathcal{T}}}^\dagger) \Theta_{\mathcal{T}} \mathbf{x}_{\mathcal{T}} \right\|_F - \|\mathbf{n}\|_F \\ &\stackrel{(e_1)}{\geq} \sqrt{1 - \delta} |\mathbf{x}(i)| - \lambda > \lambda, \end{aligned}$$

which contradicts the stopping criterion in Step 2 of Algorithm 2, where (e_1) uses the RIP property in $\mathcal{E}_{2s, \delta}$. iii) Suppose in Step 2, $\hat{\mathcal{T}}$ selects s indices, i.e., $\mathcal{T} = \hat{\mathcal{T}}$. Then $\left\| (\mathbf{I} - \Theta_{\mathcal{T}} \Theta_{\mathcal{T}}^\dagger) \mathbf{z} \right\|_F \leq \|\mathbf{n}\| \leq \lambda$ and Step 2 of Algorithm 2 will stop. Therefore, the first item in Theorem 1 is proved. We then prove the second item in Theorem 1. From $\mathcal{T} = \hat{\mathcal{T}}$, we obtain the final recovered $\hat{\mathbf{x}}$ from Algorithm 2 satisfies

$$\begin{aligned} \|\mathbf{x} - \hat{\mathbf{x}}\|_F &= \left\| \mathbf{x}_{\mathcal{T}} - \Theta_{\mathcal{T}}^\dagger (\Theta_{\mathcal{T}} \mathbf{x}_{\mathcal{T}} + \mathbf{n}) \right\|_F \\ &= \left\| \Theta_{\mathcal{T}}^\dagger \mathbf{n} \right\|_F \stackrel{(e_2)}{\leq} \frac{1}{\sqrt{1 - \delta}} \|\mathbf{n}\| \end{aligned}$$

where (e_2) uses the RIP property in $\mathcal{E}_{2s, \delta}$.

B. Proof of Lemma 2

Denote the singular value decomposition (SVD) of \mathbf{A}_i as $\mathbf{A}_i = \mathbf{U}_i \mathbf{\Sigma}_i \mathbf{V}_i^H$, where $\mathbf{U}_i \in \mathbb{C}^{R \times R}$ and $\mathbf{V}_i \in \mathbb{C}^{N_c \times R}$ are unitary matrices, i.e., $\mathbf{U}_i^H \mathbf{U}_i = \mathbf{I}$, $\mathbf{V}_i^H \mathbf{V}_i = \mathbf{I}$ and $\mathbf{\Sigma}_i = \text{diag}([\beta_{i1} \cdots \beta_{iR}])$ contain the singular values $\{\beta_{ij} \geq 0 : \forall j\}$. We first have $\sum_{j=1}^R \beta_{ij}^2 = \|\mathbf{A}_i\|_F^2 = \frac{N_c}{M}$. From i) \mathbf{n}_i is standard complex Gaussian distributed, ii) the unitary invariance property of complex Gaussian distribution, we obtain $\tilde{\mathbf{n}}_i = \mathbf{V}_i^H \mathbf{n}_i \in \mathbb{C}^{R \times 1}$ is also standard complex Gaussian distributed and is independent of \mathbf{V}_i . From (8), we have

$$\|\mathbf{n}\|_F^2 = \sum_{i=1}^M \|\mathbf{A}_i \mathbf{n}_i\|_F^2 = \sum_{i=1}^M \|\mathbf{\Sigma}_i \tilde{\mathbf{n}}_i\|_F^2 = \frac{1}{2} \sum_{i=1}^M \sum_{r=1}^R \beta_{ij}^2 \chi_2^{[ir]} \quad (23)$$

where $\{\chi_2^{[ir]} : i = 1, \dots, M, j = 1, \dots, R\}$ are i.i.d. chi-square distributed variables with 2 degrees of freedom. We first introduce the tools of sub-exponential variables from [38].

Definition 3 (Sub-Exponential Variable): X is sub-exponential with parameters (σ^2, b) if

$$\ln(\mathbb{E}[\exp(t(X - \mathbb{E}X))]) \leq \frac{t^2 \sigma^2}{2}, \quad \forall |t| < 1/b.$$

Based on the above definition, we further introduce the following properties for sub-exponential variables [38].

Lemma 3 (Properties of Sub-Exponential Variable): The following properties holds

(i) If X is sub-exponential with parameters (σ^2, b) , then X is also sub-exponential with parameters $(\bar{\sigma}^2, \bar{b})$, $\forall \bar{\sigma}^2 \geq \sigma^2$ and $\bar{b} \geq b$;

(ii) For independent sub-exponential variables X_i with parameter (σ_i^2, b_i) , $i = 1, \dots, M$, the weighted sum $X = \sum_{i=1}^M w_i X_i$ is also sub-exponential with parameters (σ^2, b) , where $\sigma^2 = \sum_{i=1}^M w_i^2 \sigma_i^2$ and $b = \max_i w_i b_i$.

(iii) For sub-exponential variables X with parameters (σ^2, b) ,

$$\Pr(X - \mathbb{E}X \geq t) \leq \begin{cases} \exp\left(-\frac{t^2}{2\sigma^2}\right) & , \quad 0 \leq t \leq \frac{\sigma^2}{b} \\ \exp\left(-\frac{t}{2b}\right) & , \quad t > \frac{\sigma^2}{b} \end{cases}.$$

Lemma 4 (Sub-exponential Property of Chi-square Variable):

Suppose χ_2 is a chi-square random variable with 2 degrees of freedom, then χ_2 is also a sub-exponential variable with parameters $(\sigma^2 = 8, b = 4)$.

Proof: Note that $\mathbb{E}(\exp((\chi_2 - \mathbb{E}(\chi_2))t)) = \frac{1}{1-2t} \exp(-2t) \leq \exp(4t^2)$, $\forall |t| \leq \frac{1}{4}$. From Definition 3, the Lemma is proved. \blacksquare

We utilize the above tools to derive the probability bound for $\|\mathbf{n}\|$. From (23) and the first two properties in Lemma 3, $\|\mathbf{n}\|_F^2 = \frac{1}{2} \sum_{i=1}^M \sum_{j=1}^R \beta_{ij}^2 \chi_2^{[ij]}$ is also a sub-exponential variable with parameters $\sigma^2 = 2 \frac{N_c}{M}$ and $b = \frac{2N_c}{M}$. From Lemma 3 (iii) and $\mathbb{E}(\|\mathbf{n}\|_F^2) = N_c$, we obtain when $\lambda^2 > 2N_c$, i.e., $t = \lambda^2 - N_c > \sigma^2/b = N_c$,

$$\Pr(\|\mathbf{n}\| \geq \lambda) \leq \exp\left(-\frac{M(\lambda^2 - N_c)}{4N_c}\right).$$

C. Proof of Theorem 2

From Theorem 1, we have

$$\begin{aligned} \Pr(\hat{\mathcal{T}} = \mathcal{T} | \mathcal{E}_{2s, \delta}) &\geq \Pr(\mathcal{E}_1 \text{ and } \|\mathbf{n}\|_F \leq \lambda) \\ &\geq 1 - \Pr(\|\mathbf{n}\|_F > \lambda) - \Pr(\bar{\mathcal{E}}_1) \\ &\geq 1 - \exp(-c_1 M) - s \cdot \left(1 - \exp\left(-\frac{2(c_2 \lambda)^2}{P_{\min}}\right)\right), \end{aligned}$$

where $\bar{\mathcal{E}}_1$ denotes the complement event of \mathcal{E}_1 in Theorem 1. From $\Pr(\hat{\mathcal{T}} = \mathcal{T}) \geq \Pr(\hat{\mathcal{T}} = \mathcal{T} | \mathcal{E}_{2s, \delta}) \Pr(\mathcal{E}_{2s, \delta})$, Theorem 2 is proved.

D. Proof of Theorem 3

We first introduce some notations and events to facilitate the proof. We then divide the proof of Theorem 3 into three parts (i.e., Lemma 5-7 below). Denote the q -th norm of a random variable X as $\mathbb{E}^q(X) \triangleq (\mathbb{E}(|X|^q))^{1/q}$ and the norm operator $\|\cdot\|_k$ as $\|\mathbf{A}\|_k = \sup_{\#\mathcal{S} \leq k} \|(\mathbf{A})_{\mathcal{S} \times \mathcal{S}}\|$, where $(\mathbf{A})_{\mathcal{S} \times \mathcal{S}}$ returns the principal submatrix with columns and row indices in \mathcal{S} . Denote

$$Z \triangleq \|\Theta^H \Theta - \mathbf{I}\|_k$$

Therefore, matrix Θ has a k -th RIP property with RIC δ (i.e., event $\mathcal{E}_{k,\delta}$) if $Z \leq \delta$ [34] and to prove $\Pr(\mathcal{E}_{k,\delta}) \geq 1 - \frac{4}{KN_c}$ in Theorem 3, it is sufficient to prove that

$$\Pr(Z > \delta) \leq \frac{4}{KN_c}. \quad (24)$$

Denote $\varphi_{max} \triangleq \frac{1}{\sqrt{MR}} \max_{i,k,c} |H_{ik}^{[c]}|$ and matrix $\mathbf{H}^{[c]}$ as

$$\mathbf{H}^{[c]} = \frac{1}{\sqrt{M}} \begin{bmatrix} H_{11}^{[c]} & H_{12}^{[c]} & \cdots & H_{1K}^{[c]} \\ H_{21}^{[c]} & H_{22}^{[c]} & \cdots & H_{2K}^{[c]} \\ \vdots & \vdots & \ddots & \vdots \\ H_{M1}^{[c]} & H_{M2}^{[c]} & \cdots & H_{MK}^{[c]} \end{bmatrix}. \quad (25)$$

Denote events \mathcal{F}_1 and \mathcal{F}_2 as:

$$\mathcal{F}_1 : \quad \varphi_{max} \leq C_3 \bar{g} \sqrt{\frac{\log(KN_c)}{MR}} \quad (26)$$

$$\mathcal{F}_2 : \quad \max_{c \in \{1, \dots, N_c\}} \|\left(\mathbf{H}^{[c]}\right)^H \mathbf{H}^{[c]} - \mathbf{I}\|_{k'} \leq \frac{C_4 \delta}{\sqrt{\log KN_c}}, \quad (27)$$

where $C_3 = \sqrt{2}e^{0.75}$, e is the natural logarithm base, C_4 ($C_4 < 1$) is a constant to be given later (Appendix F). Note that \mathcal{F}_1 and \mathcal{F}_2 depend on the channel matrices $\mathcal{H} \triangleq \{H_{ik}^{[c]} : \forall i, k, c\}$ only. Using the conditional probability property, we obtain

$$\Pr(Z > \delta) \leq \Pr(\overline{\mathcal{F}_1}) + \Pr(\overline{\mathcal{F}_2}) + \Pr(Z > \delta | \mathcal{F}_1 \mathcal{F}_2), \quad (28)$$

where $\overline{\mathcal{F}}$ denotes the complement event of \mathcal{F} . Based on (28), from the results of $\Pr(\overline{\mathcal{F}_1}) \leq \frac{1}{KN_c}$, $\Pr(\overline{\mathcal{F}_2}) \leq \frac{1}{KN_c}$ and $\Pr(Z > \delta | \mathcal{F}_1 \mathcal{F}_2) \leq \frac{2}{KN_c}$ in the following Lemma 5-7 respectively, we can obtain $\Pr(Z > \delta) \leq \frac{4}{KN_c}$. Therefore, Theorem 3 is proved.

Lemma 5 (Probability Bound I): Suppose $M \leq KN_c$. We have $\Pr(\overline{\mathcal{F}_1}) \leq \frac{1}{KN_c}$.

Proof: From [34] (equation (14)), for any q ,

$$\begin{aligned} \mathbb{E}^q(\varphi_{max}) &\leq (MKN_c)^{1/q} \max_{i,k,c} \mathbb{E}^q(|g_{ik}^{[c]} h_{ik}^{[c]}|) \\ &\leq \frac{\bar{g}(MKN_c)^{1/q}}{\sqrt{MR}} \Gamma\left(\frac{q}{2} + 1\right)^{\frac{1}{q}} \end{aligned}$$

Selecting $q = 4 \log(KN_c)$, we obtain $(MKN_c)^{1/q} \leq (KN_c)^{2/q} \leq (KN_c)^{\frac{2}{2 \log(KN_c)}} = e^{0.5}$ (and $\Gamma\left(\frac{q}{2} + 1\right)^{\frac{1}{q}} \leq \sqrt{\frac{q}{2}} = \sqrt{2 \log(KN_c)}$), hence,

$$\mathbb{E}^q(\varphi_{max}) \leq e^{0.5} \sqrt{2} \bar{g} \sqrt{\frac{\log(KN_c)}{MR}}.$$

Using the Markov's inequality, we obtain

$$\Pr\left(\varphi_{max} > \sqrt{2}e^{0.75} \bar{g} \sqrt{\frac{\log(KN_c)}{MR}}\right) \leq \left[\frac{\mathbb{E}^q(\varphi_{max})}{e^{0.25} \mathbb{E}^q(\varphi_{max})}\right]^q = \frac{1}{KN_c}$$

and hence Lemma 5 is proved. \blacksquare

Lemma 6 (Probability Bounds II): Denote $k' = \min(K, k)$. If $M \geq C_1 \delta^{-2} k' \log(KN_c) \log(2KN_c) \cdot \log\left(\frac{eK}{k'}\right)$, then

$$\Pr(\overline{\mathcal{F}_2}) \leq \frac{1}{KN_c}, \quad (29)$$

where C_1 is a constant that depends on C_4 and $L = \sqrt{2} \bar{g} \sup_{p \geq 1} 2^{\frac{1}{p}} p^{-\frac{1}{2}} \Gamma\left(\frac{p}{2} + 1\right)^{\frac{1}{p}}$ (L is a bounded constant).

Proof: See Appendix E. \blacksquare

Lemma 7 (Probability Bounds III): If $MR \geq C_2 \delta^{-2} k \log^6 KN_c$, then

$$\Pr(Z > \delta | \mathcal{F}_1 \mathcal{F}_2) \leq \frac{2}{KN_c}, \quad (30)$$

where C_2 is a constant that depends on \bar{g} .

Proof: See Appendix F. \blacksquare

E. Proof of Lemma 6

Using the probability union bound, to prove (29) in Lemma 6, it is sufficient to prove that

$$\Pr\left(\|\left(\mathbf{H}^{[c]}\right)^H \mathbf{H}^{[c]} - \mathbf{I}\|_{k'} \geq \frac{C_4 \delta}{\sqrt{\log KN_c}}\right) \leq \frac{1}{KN_c^2} \quad (31)$$

holds for each index $c \in \{1, \dots, N_c\}$. We omit the subscript of c for conciseness and prove (31) in the following. Let \mathbf{h}_k denote the k -th column of \mathbf{H} , $\forall k = 1, \dots, K$. Denote \mathcal{F}_3 as the following event:

$$\mathcal{F}_3 : \quad \max_{k \in \{1, \dots, K\}} \left| \|\mathbf{h}_k\|^2 - 1 \right| \leq \frac{C_4 \delta}{4\sqrt{\log KN_c}},$$

Using the conditional probability property, the following two equations would be sufficient to derive (31).

$$\Pr(\overline{\mathcal{F}_3}) \leq \frac{1}{2KN_c^2}. \quad (32)$$

$$\Pr\left(\|\mathbf{H}^H \mathbf{H} - \mathbf{I}\|_{k'} \geq \frac{C_4 \delta}{\sqrt{\log KN_c}} | \mathcal{F}_3\right) \leq \frac{1}{2KN_c^2}. \quad (33)$$

1) Proof of equation (32): Denote $\mathbf{h}_k = \frac{1}{\sqrt{M}} [g_{1k} h_{1k}, g_{2k} h_{2k}, \dots, g_{Mk} h_{Mk}]^T$. Then $\|\mathbf{h}_k\|^2 = \frac{1}{M} \sum_{i=1}^M |g_{ik} h_{ik}|^2 = \frac{1}{2M} \sum_i |g_{ik}|^2 \chi_2^{[i]}$, where $\{\chi_2^{[i]} : \forall i\}$ are i.i.d. chi-square random variables with 2 degrees of freedom, and $\mathbb{E}(\|\mathbf{h}_k\|^2) = 1$. From Lemma 4 and Lemma 3 (i-ii), $\|\mathbf{h}_k\|^2 = \frac{1}{2M} \sum_i |g_{ik}|^2 \chi_2^{[i]}$ is sub-exponential with parameters $(\sigma^2 = \frac{2g^2}{M}, b = \frac{2g^2}{M})$. From Lemma 3 (iii), we obtain

$$\Pr\left(\|\mathbf{h}_k\|^2 - 1 \geq \frac{C_4 \delta}{4\sqrt{\log KN_c}}\right) \leq \exp\left(-\frac{C_4 \delta^2 M}{64\bar{g}^2 \log KN_c}\right).$$

Repeating the above derivation for $-\|\mathbf{h}_k\|^2$ instead of $\|\mathbf{h}_k\|^2$, we obtain the same bound for $\Pr\left(\|\mathbf{h}_k\|^2 - 1 \leq -\frac{C_4 \delta}{4\sqrt{\log KN_c}}\right)$. Taking a union bound over different $k \in \{1, \dots, K\}$ and choosing M as $M \geq C_5 \delta^{-2} \log(KN_c) \log(2KN_c)$ with the constant $C_5 = 128\bar{g}^2$, we derive equation (32).

2) Proof of equation (33): We further introduce the following tools on sub-Gaussian variables.

Definition 4 (SubGaussian Variable [37]): A random variable X is called *sub-Gaussian* if there exists a constant C such that

$$p^{-\frac{1}{2}} (\mathbb{E}|X|^p)^{\frac{1}{p}} \leq C < \infty, \quad \forall p. \quad (34)$$

Furthermore, the *sub-Gaussian norm* of X , denoted as $\|X\|_\psi$, is defined to be the smallest L such that (34) holds, i.e., $\|X\|_\psi \triangleq \sup_{p \geq 1} p^{-\frac{1}{2}} (\mathbb{E}|X|^p)^{\frac{1}{p}}$.

Definition 5 (SubGaussian Vector [37]): A vector $\mathbf{a} \in \mathbb{C}^{m \times 1}$ is called a sub-Gaussian vector if $(\mathbf{a}^H \mathbf{x})$ is a sub-Gaussian variable for all $\|\mathbf{x}\| = 1$, $\mathbf{x} \in \mathbb{C}^{m \times 1}$. Furthermore, the sub-Gaussian norm of \mathbf{a} is defined as $\|\mathbf{a}\|_\psi = \sup_{\|\mathbf{x}\|=1} \|\mathbf{a}^H \mathbf{x}\|_\psi$. ■

In [37], a restricted isometry property (Thm 5.65) is given for matrices with SubGaussian column vectors, where each column vector has a *unit norm*. By tracking the proof, we can obtain a more general form in which each column vector is only required to be *near unit-normed*.

Lemma 8 (SubGaussian property [37]): Let \mathbf{A} be an $m \times n$ random matrix where $\mathbf{A}(1), \mathbf{A}(2), \dots, \mathbf{A}(n) \in \mathbb{C}^{m \times 1}$ are its column vectors. Suppose i) $\max_{l \in \{1, \dots, n\}} \left| \frac{1}{m} \|\mathbf{A}(l)\|^2 - 1 \right| \leq \varepsilon$, ii) $\mathbb{E}(\mathbf{A}(l)\mathbf{A}(l)^H) = \mathbf{I}_{m \times m}$, $\forall l$, and iii) the column vectors $\{\mathbf{A}(l) : \forall l\}$ are *independent* sub-Gaussian vectors. If $m \geq C_6^{[1]}(\delta - 2\varepsilon)^{-2} k' \log\left(\frac{en}{k'}\right)$, then $\|\frac{1}{m} \mathbf{A}^H \mathbf{A} - \mathbf{I}\|_{k'} > \delta$ happens with probability less than

$$2 \exp\left(-C_6^{[2]}(\delta - 2\varepsilon)^2 m\right)$$

where $0 \leq \varepsilon \leq \frac{1}{2}\delta$, $C_6^{[1]}$ and $C_6^{[2]}$ are constants that depend on L for any $L \geq \max_l \|\mathbf{A}(l)\|_\psi$.

Proof: (Sketch) The result can be easily obtained by following the proof of Thm 5.65, which is based on Thm 5.58 in [37]. In deriving the probability bound for $\|\frac{1}{m} \mathbf{A}^H \mathbf{A} - \mathbf{I}\|_{k'} > \delta$, instead of substituting $\frac{1}{m} \|\mathbf{A}(l)\|^2 = 1$ into equation (5.40) and (5.41) of [37], we shall incorporate a dynamic $1 - \varepsilon \leq \frac{1}{m} \|\mathbf{A}(l)\|^2 \leq 1 + \varepsilon$ into equation (5.41) of [37]. Using the subsequent results of equation (5.41) in [37] and proposition 5.66 of [37], Lemma 8 is obtained. ■

Note that when $\varepsilon = 0$, Lemma 8 is reduced to Thm 5.65 of [37]. First note that $\mathbb{E}(M\mathbf{h}_k\mathbf{h}_k) = \mathbf{I}$ and given \mathcal{F}_3 , $\{\mathbf{h}_k : k = 1, \dots, K\}$ are independent sub-Gaussian vectors with the sub-Gaussian norm bounded by

$$L = \max_{l \in \{1, \dots, K\}} \|\sqrt{M}\mathbf{h}_l\|_\psi \leq \bar{g} \sup_{p \geq 1} \sqrt{2} p^{-\frac{1}{2}} \Gamma\left(\frac{p}{2} + 1\right)^{\frac{1}{p}}$$

where $\sup_{p \geq 1} \sqrt{2} p^{-\frac{1}{2}} \Gamma\left(\frac{p}{2} + 1\right)^{\frac{1}{p}}$ is a bounded constant [37]. Therefore, given \mathcal{F}_3 , $\sqrt{M}\mathbf{H}$ satisfies the three conditions of \mathbf{A} in Lemma 8. Applying Lemma 8 with δ replaced by $\frac{C_4\delta}{\sqrt{\log KN_c}}$ and ε replaced by $\frac{C_4\delta}{4\sqrt{\log KN_c}}$, we obtain that when $M \geq 4C_6^{[1]}C_4^{-2}\delta^{-2} \log(KN_c)k' \log\left(\frac{eK}{k'}\right)$,

$$\Pr\left(\|\mathbf{H}^H \mathbf{H} - \mathbf{I}\|_{k'} \geq \frac{C_4\delta}{\sqrt{\log KN_c}} \mid \mathcal{F}_3\right) \leq 2 \exp\left(-\frac{C_6^{[2]}(C_4\delta)^2}{4 \log KN_c} M\right). \quad (35)$$

From equation (35), $M \geq C_1 \delta^{-2} k' \log(KN_c) \log(2KN_c) \cdot \log\left(\frac{eK}{k'}\right)$ where $C_1 = \max\left(4C_6^{[1]}C_4^{-2}, \frac{8}{C_6^{[2]}}C_4^{-2}, C_5\right)$, we derive equation (33).

F. Proof of Lemma 7

Denote the r -th row vector of Θ as $\mathbf{z}_r \in \mathbb{C}^{1 \times KN_c}$. We have

$$Z \triangleq \|\Theta^H \Theta - \mathbf{I}\|_k = \left\| \sum_{r=1}^{MR} \mathbf{z}_r^H \mathbf{z}_r - \mathbf{I} \right\|_k. \quad (36)$$

To prove $\Pr(Z > \delta \mid \mathcal{F}_1 \mathcal{F}_2) \leq \frac{2}{KN_c}$ in Lemma 7, it suffices to prove that for any given channel realization $\mathcal{H} \triangleq \{H_{ik}^{[c]} :$

$\forall i, k, c\}$ where $\mathcal{F}_1 \mathcal{F}_2$ are satisfied, the following equation is satisfied:

$$\Pr(Z > \delta \mid \mathcal{H}, \mathcal{F}_1 \mathcal{F}_2) \leq \frac{2}{KN_c}. \quad (37)$$

We then prove (37) below and the main proof flow follows from [34]. First of all, we introduce the following tools (Lemma 9-10) from [34].

Lemma 9 (Rudelson-Vershynin [34]): Suppose that $\{\mathbf{z}_r\}$ is a sequence of MR vectors in \mathbb{C}^{KN_c} , where $MR \leq KN_c$, and $\|\mathbf{z}_r\|_\infty \leq B \forall r \in \{1, \dots, MR\}$. Let $\{\xi_r \in \{-1, +1\}\}$ be an independent Rademacher series. Then

$$\mathbb{E} \left\| \sum_r \xi_r \mathbf{z}_r^H \mathbf{z}_r \right\|_k \leq \beta \left(\left\| \sum_r \mathbf{z}_r^H \mathbf{z}_r \right\|_k \right)^{\frac{1}{2}},$$

where $\beta \leq C_7 B \sqrt{k} \log^2(KN_c)$ and C_7 is an absolute constant.

Lemma 10 (Tail Probability ([34], Proposition 19)): Let $\{\mathbf{Y}_r\}$ be a sequence of independent random matrices and $\|\mathbf{Y}_r\|_k \leq B, \forall r$. Let $Y = \left\| \sum_r \mathbf{Y}_r \right\|_k$. Then

$$\Pr\{Y > C_8[u\mathbb{E}Y + tB]\} \leq e^{-u^2} + e^{-t}$$

for all $u, t \geq 1$, where C_8 is an absolute constant. ■

Denote $\mathbb{E}_{|\mathcal{H}, \mathcal{F}_1 \mathcal{F}_2}(Z) \triangleq \mathbb{E}(Z \mid \mathcal{H}, \mathcal{F}_1 \mathcal{F}_2)$ for simplicity. Based on Lemma 9-10, we obtain the following two equations

$$\mathbb{E}_{|\mathcal{H}, \mathcal{F}_1 \mathcal{F}_2}(Z) \leq \frac{C_9\delta}{\sqrt{\log KN_c}}, \quad (38)$$

$$\Pr(Z > C_{10}\delta \mid \mathcal{H}, \mathcal{F}_1 \mathcal{F}_2) \leq \frac{2}{KN_c} \quad (39)$$

where $C_9 = \left(\sqrt{\frac{16C_3^4 C_7^4 \bar{g}^4}{C_2^2}} + \sqrt{\frac{4C_3^2 C_7^2 \bar{g}^2}{C_2}} + 2C_4\right)$, $C_{10} = \left(2C_9 C_8 + \left(\frac{2C_3^2 \bar{g}^2}{C_2}\right) C_8 + 2C_9\right)$. Note that (i) equation (39) can derive our target equation (39) by properly selecting the constants C_4 and C_2 (e.g., $C_4 = \frac{1}{16(C_8+1)}$, $C_2 = \max(64(2C_8+2)^2 C_3^2 \bar{g}^2, 8C_8 C_3 \bar{g}^2)$ so that $C_{10} \leq 1$); (ii) equation (39) is derived based on equation (38). Next we focus on proving equation (38) and (39) in the following.

1) *Proof of equation (38):* Using the triangular inequality, we obtain

$$\begin{aligned} \mathbb{E}_{|\mathcal{H}, \mathcal{F}_1 \mathcal{F}_2}(Z) &\leq \underbrace{\left\| \mathbb{E}_{|\mathcal{H}, \mathcal{F}_1 \mathcal{F}_2} \left(\sum_{r=1}^{MJ} \mathbf{z}_r^H \mathbf{z}_r \right) - \mathbf{I} \right\|_k}_{\triangleq E_1} + \\ &\underbrace{\left\| \sum_{r=1}^{MJ} \left(\mathbf{z}_r^H \mathbf{z}_r - \mathbb{E}_{|\mathcal{H}, \mathcal{F}_1 \mathcal{F}_2} \left(\mathbf{z}_r^H \mathbf{z}_r \right) \right) \right\|_k}_{\triangleq E_2} \end{aligned} \quad (40)$$

From event \mathcal{F}_2 given in (27), and the fact that

$$\mathbb{E}_{|\mathcal{H}, \mathcal{F}_1 \mathcal{F}_2} \left(\sum_{r=1}^{MJ} \mathbf{z}_r^H \mathbf{z}_r \right) = \begin{bmatrix} \ddots & \mathbf{0} & & \\ \mathbf{0} & (\mathbf{H}^{[c]})^H \mathbf{H}^{[c]} & \mathbf{0} & \\ & \mathbf{0} & \ddots & \\ & & & \ddots \end{bmatrix}_{c \in \{1, 2, \dots, N_c\}}$$

We obtain $E_1 \leq \frac{C_4 \delta}{\sqrt{\log KN_c}}$. Let $\{\xi_r \in \{-1, +1\}\}$ be an independent Rademacher series [34]. We obtain,

$$\begin{aligned} E_2 &\stackrel{(a_1)}{\leq} 2\mathbb{E}_{|\mathcal{H}, \mathcal{F}_1 \mathcal{F}_2} \left\| \sum_{r=1}^{MJ} \xi_r \mathbf{z}_r^H \mathbf{z}_r \right\|_k & (41) \\ &\stackrel{(a_2)}{\leq} 2\mathbb{E}_{|\mathcal{H}, \mathcal{F}_1 \mathcal{F}_2} \left(\beta \left\| \sum_{r=1}^{MJ} \mathbf{z}_r^H \mathbf{z}_r \right\|^{\frac{1}{2}} \right) \\ &\stackrel{(a_3)}{\leq} 2 \left[\mathbb{E}_{|\mathcal{H}, \mathcal{F}_1 \mathcal{F}_2} (\beta^2) \right]^{1/2} (\mathbb{E}_{|\mathcal{H}, \mathcal{F}_1 \mathcal{F}_2} (Z) + 1)^{1/2} \end{aligned}$$

where (a₁) uses the symmetrization property (i.e., Lemma 5.46 of [37]), (a₂) uses the Rudelson-Vershynin Lemma and (a₃) comes from the Cauchy-Schwarz inequality. When $\mathcal{F}_1 \mathcal{F}_2$ happens, we obtain $\|\mathbf{z}_r\|_\infty \leq C_3 \bar{g} \sqrt{\frac{\log(KN_c)}{MR}}$, $\forall r$ and hence

$$\left[\mathbb{E}_{|\mathcal{H}, \mathcal{F}_1 \mathcal{F}_2} (\beta^2) \right]^{1/2} \leq C_7 C_3 \bar{g} \sqrt{\frac{k \log^5(KN_c)}{MR}} \leq \frac{C_7 C_3 \bar{g} \delta}{\sqrt{C_2 \log KN_c}}$$

in (41). Suppose $C_2 \geq C_7^2 C_3^2 \bar{g}^2$ so that $\frac{C_7 C_3 \bar{g} \delta}{\sqrt{C_2 \log KN_c}} \leq \frac{\delta}{\sqrt{\log KN_c}}$. From (40) and (41), we obtain

$$\mathbb{E}_{|\mathcal{H}, \mathcal{F}_1 \mathcal{F}_2} (Z) \leq \frac{C_4 \delta}{\sqrt{\log KN_c}} + \frac{2C_7 C_3 \bar{g} \delta}{\sqrt{C_2 \log KN_c}} (\mathbb{E}_{|\mathcal{H}, \mathcal{F}_1 \mathcal{F}_2} (Z) + 1)^{1/2}$$

which further derives our target equation (38).

2) *Proof of equation (39)*: We prove (39) based on (38). First, define the symmetrized random variable

$$\mathbf{Y}_r = \varepsilon_r (\mathbf{z}_r^H \mathbf{z}_r - \tilde{\mathbf{z}}_r^H \tilde{\mathbf{z}}_r), \quad Y = \left\| \sum_{r=1}^{MJ} \varepsilon_r (\mathbf{z}_r^H \mathbf{z}_r - \tilde{\mathbf{z}}_r^H \tilde{\mathbf{z}}_r) \right\|_k$$

where $\{\varepsilon_r : r = 1, \dots, MR\}$ are an i.i.d. Rademacher sequence and $\tilde{\mathbf{z}}_r$ is an independent copy of \mathbf{z}_r . Therefore,

$$\mathbb{E}_{|\mathcal{H}, \mathcal{F}_1 \mathcal{F}_2} Y \leq 2\mathbb{E}_{|\mathcal{H}, \mathcal{F}_1 \mathcal{F}_2} (Z) \leq \frac{2C_9 \delta}{\sqrt{\log(KN_c)}}.$$

From the symmetrization property (i.e., equation (6.1) in [39]), we obtain

$$\Pr(Z > 2\mathbb{E}(Z) + u \mid \mathcal{H}, \mathcal{F}_1 \mathcal{F}_2) \leq 2\mathbb{P}(Y > u \mid \mathcal{H}, \mathcal{F}_1 \mathcal{F}_2). \quad (42)$$

On the other hand, given $\mathcal{F}_1 \mathcal{F}_2$, we have,

$$\begin{aligned} \max_r \|\mathbf{Y}_r\|_k &= \max_r \|\mathbf{z}_r^H \mathbf{z}_r - \tilde{\mathbf{z}}_r^H \tilde{\mathbf{z}}_r\|_k \leq 2 \max_r \|\mathbf{z}_r^H \mathbf{z}_r\|_k \\ &\leq 2k\varphi_{max}^2 \leq 2C_3^2 \bar{g}^2 \frac{k \log(KN_c)}{MR} \leq \left(\frac{2C_3^2 \bar{g}^2}{C_2} \right) \frac{\delta}{\log(KN_c)} \end{aligned}$$

Note that under a given realization \mathcal{H} , different rows vectors $\{\mathbf{z}_r : \forall r\}$ are independent from (12) and hence $\{\mathbf{Y}_r : \forall r\}$ are also independent. Therefore, the tail probability property in Lemma 10 can be applied. Applying Lemma 10 with $u = \sqrt{\log(KN_c)}$ and $t = \log(KN_c)$, using equation (42), we obtain

$$\begin{aligned} &\Pr \left(Z > \left(2C_9 C_8 + \left(\frac{2C_3^2 \bar{g}^2}{C_2} \right) C_8 + 2C_9 \right) \delta \mid \mathcal{H}, \mathcal{F}_1 \mathcal{F}_2 \right) \\ &\leq 2\Pr \left(Y > \left(2C_9 C_8 + \left(\frac{2C_3^2 \bar{g}^2}{C_2} \right) \right) \delta \mid \mathcal{H}, \mathcal{F}_1 \mathcal{F}_2 \right) \\ &\leq 2\Pr \left(Y > C_3 \left\{ u \mathbb{E}_{|\mathcal{H}, \mathcal{F}_1 \mathcal{F}_2} Y + t \frac{\delta}{\log(KN_c)} \right\} \mid \mathcal{H}, \mathcal{F}_1 \mathcal{F}_2 \right) \\ &\leq 2e^{-\log(KN_c)} = \frac{2}{KN_c}. \end{aligned} \quad (43)$$

and hence equation (39) is obtained.

G. Proof of Theorem 4

First, we can always upper bound the average data rate by the capacity obtained in the ideal case in which the signal support of \mathbf{x} is correct, i.e., $\hat{\mathcal{T}} = \mathcal{T}$. Therefore,

$$\mathbb{E}(R_{sum}) \leq \mathbb{E} \left(\sum_{i=1}^s \log \left(1 + \frac{P}{\alpha_i} \right) \right). \quad (44)$$

where $\{\alpha_i : i = 1, \dots, s\}$ are the diagonal elements of the Hermitian matrix $\Psi = (\Theta_{\mathcal{T}})^\dagger (\mathbf{A} \mathbf{A}^H) ((\Theta_{\mathcal{T}})^\dagger)^H$. Denote the SVD of \mathbf{A}_i as $\mathbf{A}_i = \mathbf{U}_i \Sigma_i \mathbf{V}_i^H$, as in Appendix B, where $\mathbf{U}_i \in \mathbb{C}^{R \times R}$ and $\mathbf{V}_i \in \mathbb{C}^{N_c \times R}$ are unitary matrices and $\Sigma_i \in \mathbb{C}^{R \times R}$ is the diagonal matrix with singular values. Denote

$$\mathbf{H} = [\mathbf{H}_1^T \quad \dots \quad \mathbf{H}_M^T]^T, \quad \mathbf{V} = \text{diag}([\mathbf{V}_1 \quad \dots \quad \mathbf{V}_M]).$$

We obtain $\Psi = (\mathbf{H}_7^H \mathbf{V} \mathbf{V}^H \mathbf{H}_7)^{-1}$, and hence $\sum \frac{1}{\alpha_i} = \text{tr}(\mathbf{H}_7^H \mathbf{V} \mathbf{V}^H \mathbf{H}_7)$. From the generation method of \mathbf{A}_i in Definition 1, $\mathbf{V}_i^H \mathbf{P}_i$ has the same distribution as \mathbf{V}_i and is independent of \mathbf{P}_i for any permutation matrix $\mathbf{P}_i \in \mathbb{C}^{N_c \times N_c}$. Denote $\mathbf{P} = \text{diag}([\mathbf{P}_1 \quad \dots \quad \mathbf{P}_M])$. We obtain

$$\mathbb{E} \sum_{i=1}^s \frac{1}{\alpha_i} = \text{tr} \left(\mathbb{E}(\mathbf{V} \mathbf{V}^H) \mathbb{E}(\mathbf{P}^H \mathbf{H}_7 \mathbf{H}_7^H \mathbf{P}) \right) = \frac{sMR}{N_c} = sM\alpha. \quad (45)$$

Based on (44) and (45), from the Jensen's inequality and the concavity of function $h(x) = \log(1+x)$, we obtain

$$\mathbb{E} \left(\sum_{i=1}^s \log \left(1 + P \left(\frac{1}{\alpha_i} \right) \right) \right) \leq s \log(1 + M\alpha P),$$

and hence the upper bound is obtained. Next, we prove the lower bound. From Theorem 2, when $P \gg 4c_2^2 N_c$ and $\lambda = \left(\frac{PN_c}{4c_2^2} \right)^{\frac{1}{4}}$, $\Pr(\hat{\mathcal{T}} = \mathcal{T}) \geq \Pr(\mathcal{E}_{2s, \delta})$ and we obtain

$$\mathbb{E}(R_{sum}) \geq \Pr(\mathcal{E}_{2s, \delta}) \cdot \mathbb{E} \left[\sum_{i=1}^s \log \left(1 + \frac{P}{\alpha_i} \right) \mid \mathcal{E}_{2s, \delta} \right] \quad (46)$$

where $\{\alpha_i : i = 1, \dots, s\}$ are the diagonal elements of the Hermitian matrix $\Psi = (\Theta_{\mathcal{T}})^\dagger (\mathbf{A} \mathbf{A}^H) ((\Theta_{\mathcal{T}})^\dagger)^H$. Based on (46), to prove the lower bound in Theorem 4, it is sufficient to prove that

$$\mathbb{E} \left[\sum_{i=1}^s \log \left(1 + \frac{P}{\alpha_i} \right) \mid \Theta, \mathcal{E}_{2s, \delta} \right] \geq s \log(1 + (1 - \delta)M\alpha P). \quad (47)$$

We then prove (47) in the following. Note that given Θ and $\mathcal{E}_{2s, \delta}$, the conditional distribution of $\mathbf{P} \mathbf{A}$ is the same as \mathbf{A} for any diagonal matrix $\mathbf{P} \in \mathbb{C}^{MR \times MR}$ where the diagonal elements of \mathbf{P} are randomly drawn from $\{-1, 1\}$ with equal probability. Therefore, we obtain

$$\mathbb{E}(\mathbf{A} \mathbf{A}^H \mid \Theta, \mathcal{E}_{2s, \delta}) = \mathbb{E}(\mathbf{P} \mathbf{A} \mathbf{A}^H \mathbf{P} \mid \Theta, \mathcal{E}_{2s, \delta}) = \frac{1}{M\alpha} \mathbf{I}.$$

Based on this equation, we further obtain

$$\begin{aligned} &\mathbb{E} \left(\sum_{i=1}^s \alpha_i \mid \Theta, \mathcal{E}_{2s, \delta} \right) = \mathbb{E}(\text{tr}(\Psi) \mid \Theta, \mathcal{E}_{2s, \delta}) \\ &= \text{tr} \left((\Theta_{\mathcal{T}})^\dagger \mathbb{E}(\mathbf{A} \mathbf{A}^H \mid \Theta, \mathcal{E}_{2s, \delta}) ((\Theta_{\mathcal{T}})^\dagger)^H \right) \\ &= \frac{1}{M\alpha} \text{tr} \left(((\Theta_{\mathcal{T}}^H \Theta_{\mathcal{T}})^{-1}) \right) \stackrel{(d)}{\leq} \frac{s}{(1 - \delta)M\alpha} \end{aligned} \quad (48)$$

where (d) comes from the fact that the s eigenvalues of the Hermitian matrix $\Theta_{\mathcal{T}}^H \Theta_{\mathcal{T}}$ are bounded in $[1 - \delta, 1 + \delta]$ from the RIP condition (i.e., $\mathcal{E}_{2s, \delta}$) of Θ . Based on (48), from the Jensen's inequality and the convexity of function $h(x) = \log(1 + \frac{1}{x})$, $\forall x > 0$, we derive (47). Therefore, the lower bound of $\mathbb{E}(R_{sum})$ is proved.

REFERENCES

- [1] A. Tolli, M. Codreanu, and M. Juntti, "Cooperative MIMO-OFDM cellular system with soft handover between distributed base station antennas," *IEEE Trans. Wireless Commun.*, vol. 7, no. 4, pp. 1428–1440, 2008.
- [2] C.-X. Wang, X. Hong, X. Ge, X. Cheng, G. Zhang, and J. Thompson, "Cooperative MIMO channel models: a survey," *IEEE Commun. Mag.*, vol. 48, no. 2, pp. 80–87, 2010.
- [3] C. Mobile, "C-RAN: the road towards green RAN," *White Paper, ver. vol. 2*, 2011.
- [4] P. Chanclou, A. Pizzinat, F. Le Clech, T.-L. Reedeker, Y. Lagadec, F. Saliou, B. Le Guyader, L. Guillo, Q. Deniel, S. Gosselin *et al.*, "Optical fiber solution for mobile fronthaul to achieve cloud radio access network," in *Future Network and Mobile Summit (FutureNetworkSummit)*, 2013. IEEE, 2013, pp. 1–11.
- [5] C. J. Bernardos, A. De Domenico, J. Ortin, P. Rost, and D. Wubben, "Challenges of designing jointly the backhaul and radio access network in a cloud-based mobile network," in *Future Network and Mobile Summit (FutureNetworkSummit)*, 2013. IEEE, 2013, pp. 1–10.
- [6] C. T. Ng and H. Huang, "Linear precoding in cooperative MIMO cellular networks with limited coordination clusters," *IEEE J. Sel. Areas Commun.*, vol. 28, no. 9, pp. 1446–1454, 2010.
- [7] M. Hong, R. Sun, H. Baligh, and Z.-Q. Luo, "Joint base station clustering and beamformer design for partial coordinated transmission in heterogeneous networks," *IEEE J. Sel. Areas Commun.*, vol. 31, no. 2, pp. 226–240, Feb. 2013.
- [8] Y. Zhou and W. Yu, "Optimized backhaul compression for uplink cloud radio access network," *IEEE J. Sel. Areas Commun.*, vol. 32, no. 6, pp. 1295–1307, June 2014.
- [9] S.-H. Park, O. Simeone, O. Sahin, and S. Shamai, "Robust layered transmission and compression for distributed uplink reception in cloud radio access networks," *IEEE Trans. Veh. Technol.*, vol. 63, no. 1, pp. 204–216, Jan. 2014.
- [10] —, "Robust and efficient distributed compression for cloud radio access networks," *IEEE Trans. Veh. Technol.*, vol. 62, no. 2, pp. 692–703, 2013.
- [11] A. Del Coso and S. Simoens, "Distributed compression for MIMO coordinated networks with a backhaul constraint," *IEEE Trans. Wireless Commun.*, vol. 8, no. 9, pp. 4698–4709, 2009.
- [12] M. Yun, Y. Rong, Y. Zhou, H.-A. Choi, J.-H. Kim, J. Sohn, and H.-I. Choi, "Analysis of uplink traffic characteristics and impact on performance in mobile data networks," in *Proc. IEEE Int. Conf. Commun. (ICC)*. IEEE, 2008, pp. 4564–4568.
- [13] V. 3GPP TS 22.368, "Service requirements for machine-type communications," 3GPP ETSI, Tech. Rep., June 2012. [Online]. Available: <http://www.3gpp.org/DynaReport/36211.htm>
- [14] M. Hasan, E. Hossain, and D. Niyato, "Random access for machine-to-machine communication in LTE-advanced networks: issues and approaches," *IEEE Commun. Mag.*, vol. 51, no. 6, 2013.
- [15] A. Laya, L. Alonso, and J. Alonso-Zarate, "Is the random access channel of LTE and LTE-A suitable for M2M communications? A survey of alternatives," *IEEE Commun. Surveys & Tutorials*, vol. 16, no. 1, pp. 4–16, First 2014.
- [16] H. Zhu and G. Giannakis, "Sparsity-embracing multiuser detection for CDMA systems with low activity factory," in *Proc. IEEE Int. Symp. Information Theory (ISIT)*, July 2009, pp. 164–168.
- [17] H. F. Schepker and A. Dekorsy, "Sparse multi-user detection for CDMA transmission using greedy algorithms," in *Proc. IEEE Int. Symp. Wireless Commun. Systems (ISWCS)*. IEEE, 2011, pp. 291–295.
- [18] H. Zhu and G. B. Giannakis, "Exploiting sparse user activity in multiuser detection," *IEEE Trans. Commun.*, vol. 59, no. 2, pp. 454–465, 2011.
- [19] D. Baron, M. F. Duarte, M. B. Wakin, S. Sarvotham, and R. G. Baraniuk, "Distributed compressive sensing," *arXiv preprint arXiv:0901.3403*, 2005. [Online]. Available: <http://arxiv.org/abs/0901.3403>
- [20] E. Candes and T. Tao, "Decoding by linear programming," *IEEE Trans. Inf. Theory*, vol. 51, no. 12, pp. 4203–4215, 2005.
- [21] E. J. Candès and M. B. Wakin, "An introduction to compressive sampling," *IEEE Signal Process. Mag.*, vol. 25, no. 2, pp. 21–30, 2008.
- [22] Y. Wang, A. Pandharipande, Y. L. Polo, and G. Leus, "Distributed compressive wide-band spectrum sensing," in *Proc. Inf. Theory and Applications Workshop*. IEEE, 2009, pp. 178–183.
- [23] R. 3GPP TS 36.211, "Evolved universal terrestrial radio access (E-UTRA); physical channels and modulation," 3GPP ETSI, Tech. Rep., 2010. [Online]. Available: <http://www.3gpp.org/DynaReport/36211.htm>
- [24] Y. Wu, G. Min, K. Li, and B. Javadi, "Modeling and analysis of communication networks in multicenter systems under spatio-temporal bursty traffic," *IEEE Trans. Parallel and Distributed Systems*, vol. 23, no. 5, pp. 902–912, 2012.
- [25] H. Huang, S. Misra, W. Tang, H. Barani, and H. Al-Azzawi, "Applications of compressed sensing in communications networks," *arXiv preprint arXiv:1305.3002*, 2013. [Online]. Available: <http://arxiv.org/abs/1305.3002>
- [26] P. Zador, "Asymptotic quantization error of continuous signals and the quantization dimension," vol. 28, no. 2, pp. 139–149, 1982.
- [27] W. Dai and O. Milenkovic, "Information theoretical and algorithmic approaches to quantized compressive sensing," *IEEE Trans. Commun.*, vol. 59, no. 7, pp. 1857–1866, 2011.
- [28] J. A. Tropp and A. C. Gilbert, "Signal recovery from random measurements via orthogonal matching pursuit," *IEEE Trans. Inf. Theory*, vol. 53, no. 12, pp. 4655–4666, 2007.
- [29] D. Needell and J. A. Tropp, "CoSaMP: Iterative signal recovery from incomplete and inaccurate samples," *Applied and Computational Harmonic Analysis*, vol. 26, no. 3, pp. 301–321, 2009.
- [30] W. Dai and O. Milenkovic, "Subspace pursuit for compressive sensing signal reconstruction," *IEEE Trans. Inf. Theory*, vol. 55, no. 5, pp. 2230–2249, 2009.
- [31] Y. Jiang, M. K. Varanasi, and J. Li, "Performance analysis of ZF and MMSE equalizers for MIMO systems: an in-depth study of the high snr regime," *IEEE Trans. Inf. Theory*, vol. 57, no. 4, pp. 2008–2026, 2011.
- [32] S. Boucheron, G. Lugosi, and O. Bousquet, "Concentration inequalities," in *Advanced Lectures on Machine Learning*. Springer, 2004, pp. 208–240.
- [33] R. Baraniuk, M. Davenport, R. DeVore, and M. Wakin, "A simple proof of the restricted isometry property for random matrices," *Constructive Approximation*, vol. 28, no. 3, pp. 253–263, 2008.
- [34] J. Tropp, J. Laska, M. Duarte, J. Romberg, and R. Baraniuk, "Beyond nyquist: Efficient sampling of sparse bandlimited signals," *IEEE Trans. Inf. Theory*, vol. 56, no. 1, pp. 520–544, Jan. 2010.
- [35] J. Haupt, W. U. Bajwa, G. Raz, and R. Nowak, "Toeplitz compressed sensing matrices with applications to sparse channel estimation," *IEEE Trans. Inf. Theory*, vol. 56, no. 11, pp. 5862–5875, 2010.
- [36] G. Raskutti, M. J. Wainwright, and B. Yu, "Restricted eigenvalue properties for correlated gaussian designs," *The Journal of Machine Learning Research*, vol. 11, pp. 2241–2259, 2010.
- [37] R. Vershynin, "Introduction to the non-asymptotic analysis of random matrices," *arXiv preprint arXiv:1011.3027*, 2010. [Online]. Available: <http://arxiv.org/abs/1011.3027>
- [38] P. Bartlett, *Theoretical Statistics, Lecture 3*. UC Berkeley. [Online]. Available: <http://www.stat.berkeley.edu/~bartlett/courses/2013spring-stat210b/notes/3notes.pdf>
- [39] N. Vakhania, V. Tarieladze, and S. Chobanyan, *Probability distributions on Banach spaces*. Springer, 1987, vol. 14.